JPL PUBLICATION 79-93

Spectral Characteristics of Convolutionally Coded Digital Signals

Dariush Divsalar
Marvin K. Simon

August 1, 1979

National Aeronautics and
Space Administration

Jet Propulsion Laboratory
California Institute of Technology
Pasadena, California

JPL PUBLICATION 79-93

Spectral Characteristics of Convolutionally Coded Digital Signals

Dariush Divsalar
Marvin K. Simon

August 1, 1979

National Aeronautics and
Space Administration

Jet Propulsion Laboratory
California Institute of Technology
Pasadena, California

TABLE OF CONTENTS

LIST OF FIGURES

Figures

LIST OF FIGURES (contd)

Figures

ABSTRACT

The power spectral density of the output symbol sequence of a convolutional encoder is computed for two different input symbol stream source models, namely, an NRZ signaling format and a first order Markov source. In the former, the two signaling states of the binary waveform are not necessarily assumed to occur with equal probability. The effects of alternate symbol inversion on this spectrum are also considered. The mathematical results are illustrated with many examples corresponding to optimal performance codes. It is demonstrated that only for the case of a purely random input source (e.g., NRZ data with equiprobable symbols), and a particular class of codes, is the output spectrum identical to the input spectrum except for a frequency scaling (expansion) by the reciprocal of the code rate. In all other cases, the output spectrum is sufficiently changed relative to the input spectrum that the commonly quoted statement "a convolutional encoder produces a bandwidth expansion by a factor equal to the reciprocal of the code rate" must be exercised with care.

I. Introduction

While much attention has been paid toward constructing convolutional codes that achieve optimum error probability performance, very little attention, if any, has been paid toward examining the spectral properties of the corresponding encoder outputs. Perhaps the reason for this is that for most of the optimum performance codes found thus far, the output encoder spectrum, corresponding to a random NRZ input, is merely a frequency scaled version of the input $(\sin x/x)^2$ spectrum. Stated another way, a purely random input gives a purely random output with a bandwidth expansion equal to the reciprocal of the code rate.

In this report, we first examine the conditions (class of codes) for which the above is not a true statement. Indeed, it is shown that some of the optimum performance codes fall into this category. In these instances, the bandwidth expansion produced by the encoder can be considerably less than the reciprocal of the code rate. A discussion of the implications of this statement will be given in Section VII titled "Observations and Conclusions."

Following the above considerations, we determine the spectral characteristics of the convolutional encoder output when the input is not a purely random NRZ source. First, we generalize to the case where the input still has an NRZ format; however, the two signaling states of the binary waveform are not assumed to occur with equal probability, i.e., a so-called unbalanced NRZ source. Since an unbalanced NRZ source has a symbol transition density which is less than 1/2, we next generalize to a first-order Markov input which allows symbol transition densities anywhere between 0 and 1. Finally, the effects of alternate symbol inversion on encoder output spectrum are considered.

We begin the report by noting that the symbol sequence at the output of a convolutional encoder is a cyclostationary process (Ref. 1) with period equal to the number of output interleaving taps. After defining the general model of a convolutional encoder, we then give a general expression for the spectrum of a cyclostationary process and show how it is applied to the convolutional encoder output sequence. From this point on, the report focuses on all of the special cases brought out in the above discussion.

II. Convolutional Encoder Model

Consider a convolutional encoder with constraint length K and rate b/n, as shown in Fig. 1. In the mth information interval, b information symbols a_{mb+j}; $j = 0, 1, 2, \ldots,$ b-1 enter the encoder and n channel symbols X_{mn+p}; $p = 1, 2, \ldots,$ n exit the encoder. The structure of such a convolutional encoder can also be defined by a generator (connection) matrix, namely

$$\underline{G} = \begin{bmatrix} g_{1,1}\, g_{1,2} \cdots\cdots g_{1,Kb} \\ g_{2,1}\, g_{2,2} \cdots\cdots g_{2,Kb} \\ \vdots \\ g_{n,1}\, g_{n,2} \cdots\cdots g_{n,Kb} \end{bmatrix}$$

where $g_{i,j}$ is either one or zero depending, respectively, on whether the ith modulo summer is connected to the jth shift register stage. For mathematical convenience, we shall assume that both the input symbols $\{a_{mb+j}\}$ and the output symbols $\{X_{mn+p}\}$ take on values plus and minus one. This allows modulo 2

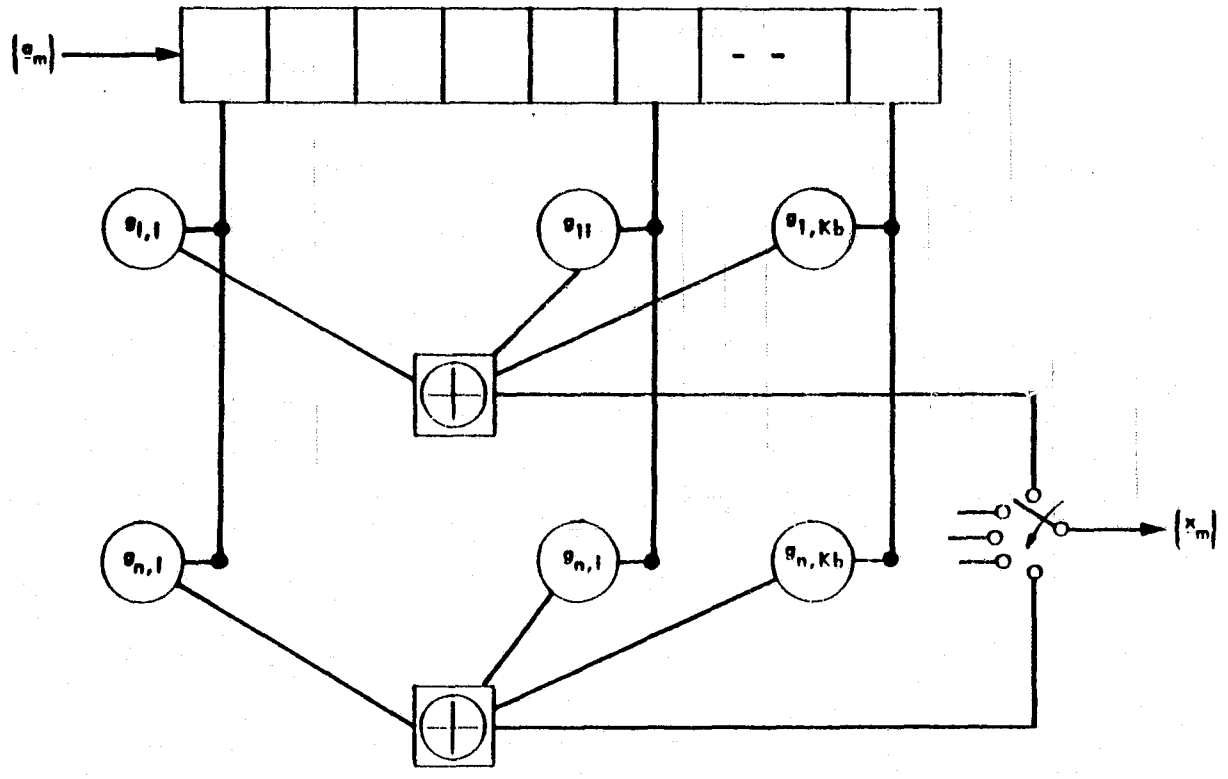

Figure 1. A general constraint length K, rate b/n convolutional code

summation operations to be replaced by algebraic products. Thus, the encoder of Fig. 1 has the input-output relation

$$X_{mn+p} = \prod_{i=1}^{Kb} \left[a_{(m+1)b-i}\right]^{g_{p,i}} \tag{1}$$

Clearly the output sequence $\{X_{mn+p}\}$ is cyclostationary with period n.

III. Spectrum of a Cyclostationary Pulse Stream

By definition (Ref. 1), a sequence is cyclostationary with period n, if for any p and λ

$$E\{X_{mn+p}\} = E\{X_p\} \tag{2}$$

and

$$E\{X_{mn+p}\, X_{mn+p+\lambda}\} = E\{X_p X_{p+\lambda}\}\,; \quad m = 0, \pm 1, \pm 2, \ldots\ldots \tag{3}$$

If, from the sequence $\{X_i\}$, we form a synchronous data pulse stream

$$m(t) = \sum_{i=-\infty}^{\infty} X_i\, p(t-iT) \tag{4}$$

where p(t) is the elementary signal (pulse shape), then the continuous component of the power spectral density of m(t) can be expressed in the form (Appendix A)

$$S_c(f) = S_p(f)\, S_X(f) \tag{5}$$

where $S_p(f)$ is a pulse shape factor defined by

$$S_p(f) = \frac{1}{T}\left|P(f)\right|^2 \tag{6}$$

with P(f) the Fourier transform of p(t) and

$$S_X(f) = \frac{1}{n}\sum_{p=1}^{n}\left[\sum_{\lambda=-\infty}^{\infty} \operatorname{cov}(X_p, X_{p+\lambda})\, e^{-j2\pi\lambda fT}\right] \tag{7}$$

In (7), $\text{cov}\,(X_p, X_{p+\lambda})$ is the covariance function of the sequence $\{X_i\}$ defined by

$$\text{cov}\,(X_p, X_{p+\lambda}) = \overline{(X_p - \overline{X}_p)\,(X_{p+\lambda} - \overline{X}_{p+\lambda})} \tag{8}$$

and the overbar denotes expectation.

Letting

$$\lambda = n\ell + q - p\,; \quad q = 1, 2, \ldots, n \tag{9}$$

then we can rewrite equation (7) as

$$S_X(f) = \frac{1}{n} \sum_{p=1}^{n} \sum_{q=1}^{n} \sum_{\ell=-\infty}^{\infty} \text{cov}\,(X_p, X_{n\ell+q})\, e^{-j2\pi(n\ell+q-p)fT} \tag{10}$$

Eq. (10) will be more useful later, since it shows that X_p is the symbol generated from the p^{th} interleaving tap output and $X_{n\ell+q}$ is the symbol generated from the q^{th} interleaving tap output.

From (2) and (3) we note that

$$\text{cov}\,(X_p, X_{n\ell+q}) = \text{cov}\,(X_{p-n\ell}, X_q) \tag{11}$$

Thus, using (11), we can rewrite (10) in the more compact form

$$S_X(f) = \frac{1}{n} \sum_{p=1}^{n} \sum_{q=1}^{n} \sum_{\ell=0}^{\infty} \epsilon_\ell\, \text{cov}\,(X_p, X_{n\ell+q}) \cos\left[2\pi(n\ell + q - p)\, fT\right] \tag{12}$$

where ϵ_ℓ is the Neumann factor defined by

$$\epsilon_\ell = \begin{cases} 1\ ; & \ell = 0 \\ 2\ ; & \text{otherwise} \end{cases} \tag{13}$$

We shall define the "memory" of the cyclostationary process as the smallest integer ℓ^* such that $\text{cov}\,(X_p\, X_{n\ell+q}) = 0$ for $\ell > \ell^*$.

If $\{X_i\}$ is not zero mean, then in addition to the continuous power spectrum of (5), it will also have a discrete spectral component $S_d(f)$, which is given (Appendix A) as

$$S_d(f) = \frac{1}{(nT)^2} \sum_{k=-\infty}^{\infty} \left| P\left(\frac{k}{nT}\right)\right|^2 \left(\sum_{i=1}^{n} \overline{X}_i\, e^{-j\frac{2\pi ik}{n}}\right) \cdot$$

$$\times \left(\sum_{m=1}^{n} \overline{X}_m\, e^{j\frac{2\pi mk}{n}}\right) \delta\left(f - \frac{k}{nT}\right) \tag{14}$$

which after some simplification can be reduced to

$$S_d(f) = \frac{1}{(nT)^2} \sum_{k=-\infty}^{\infty} \left| P\left(\frac{k}{nT}\right)\right|^2 \left\{\left[\sum_{m=1}^{n} \overline{X}_m \cos\left(\frac{2\pi mk}{m}\right)\right]^2\right.$$

$$\left. + \left[\sum_{m=1}^{n} \overline{X}_m \sin\left(\frac{2\pi mk}{n}\right)\right]^2\right\} \delta\left(f - \frac{k}{nT}\right) \tag{15}$$

IV. Encoder Output Spectrum for Independent Binary Symbol Input

Consider the input to the encoder of Fig. 1 to be a sequence of independent binary symbols $\{a_j\}$ that take on values ± 1 with probabilities

$$\Pr\{a_j = -1\} = 1 - \Pr\{a_j = 1\} = p^* \tag{16a}$$

and average symbol value

$$E\{a_j\} = 1 - 2p^* \triangleq \bar{a} \tag{16b}$$

The transition probability which characterizes this sequence is then

$$p_t = 2p^*(1 - p^*) \tag{17}$$

Letting $m = 0$ in (1) with no loss in generality, then since for independent random variables, the expectation of their product equals the product of their expectations, we have

$$\overline{X}_p = (\bar{a})^{\alpha_p} = (1 - 2p^*)^{\alpha_p}; \quad p = 1, 2, \ldots, n \tag{18}$$

where

$$\alpha_p \triangleq \sum_{i=1}^{Kb} g_{p,i} \tag{19}$$

i.e., the algebraic sum of the number of +1's in the pth row of $\underline{G}$. Furthermore, it can be shown that

$$\operatorname{cov}\left(X_p,\ X_{n\ell+q}\right) = \begin{cases} (\bar{a})^{\alpha_p+\alpha_q-2\beta_{pq}(\ell)} - (\bar{a})^{\alpha_p+\alpha_q}; & 0 \le \ell \le K-1 \\ (\bar{a})^{\alpha_q+\alpha_p-2\beta_{qp}(-\ell)} - (\bar{a})^{\alpha_q+\alpha_p}; & -(K-1) \le \ell \le 0 \\ 0\ ; \quad \text{otherwise} \end{cases} \tag{20}$$

where

$$\beta_{pq}(\ell) \triangleq \sum_{i=1}^{(K-\ell)b} g_{p,i}\, g_{q,i+\ell b} \tag{21}$$

i.e., the cross correlation of the pth row* of $\underline{G}$ with the qth row shifted by ℓb elements. Finally, substituting (18) and (20) into (12) and (15) gives the desired results for the continuous and discrete components of the encoder output spectrum, namely

$$S_X(f) = \frac{1}{n} \sum_{p=1}^{n} \sum_{q=1}^{n} \sum_{\ell=0}^{K-1} \epsilon_\ell \left[(\bar{a})^{\alpha_p+\alpha_q-2\beta_{pq}(\ell)} - (\bar{a})^{\alpha_p+\alpha_q} \right]$$

$$\times \cos\left[2\pi\,(n\ell + q - p)\, fT\right]$$

$$S_c(f) = T\left(\frac{\sin \pi fT}{\pi fT}\right)^2 S_X(f) \tag{22}$$

*The cross correlation is performed only on the parts of the pth and shifted qth rows whose elements overlap.

and

$$S_d(f) = \frac{1}{n^2} \sum_{k=-\infty}^{\infty} \left(\frac{\sin \frac{\pi k}{n}}{\frac{\pi k}{n}} \right)^2 \left\{ \left[\sum_{m=1}^{n} (\bar{a})^{\alpha_m} \cos \left(\frac{2\pi mk}{n} \right) \right]^2 \right.$$

$$\left. + \left[\sum_{m=1}^{n} (\bar{a})^{\alpha_m} \sin \left(\frac{2\pi mk}{n} \right) \right]^2 \right\} \delta \left(f - \frac{k}{nT} \right) \tag{23}$$

In (22) and (23), we have also assumed that p(t) is a unit rectangular pulse so that the shape factor of (6) is given by

$$S_p(f) = T \left(\frac{\sin \pi fT}{\pi fT} \right)^2 \tag{24}$$

Note that the results in (22) and (23) are functions of only: (1) the a priori symbol probability p* [through $\bar{a}$ of (16)] and (2) the sums and cross correlations of the rows of the generator matrix $\underline{G}$ [through (19) and (21)].

Several interesting points can be deduced from (22). First, note from (19) and (21) that for p = q and $\ell = 0$, the exponent $\alpha_p + \alpha_q - 2\beta_{pq}(\ell) = 0$ independent of the code. Thus, for these terms

$$(\bar{a})^{\alpha_p + \alpha_q - 2\beta_{pq}(\ell)} = 1 \tag{25}$$

for all $\bar{a}$ (including zero). It is also possible that the above exponent can be zero for other combinations of p, q, and ℓ. To see the class of codes for

which this can be true, we first rewrite the exponent in a different form. From (19) and (21)

$$\alpha_p + \alpha_q - 2\beta_{pq}(\ell) = \sum_{i=1}^{Kb} (g_{p,i} + g_{q,i}) - 2 \sum_{i=1}^{(K-\ell)b} g_{p,i}\, g_{q,i+\ell b}$$

$$= \sum_{i=(K-\ell)b+1}^{Kb} g_{p,i} + \sum_{i=1}^{\ell b} g_{q,i}$$

$$+ \sum_{i=1}^{(K-\ell)b} \left[g_{p,i} + g_{q,i+\ell b} - 2 g_{p,i}\, g_{q,i+\ell b} \right]$$

$$= \sum_{i=(K-\ell)b+1}^{Kb} g_{p,i} + \sum_{i=1}^{\ell b} g_{q,i}$$

$$+ \sum_{i=1}^{(K-\ell)b} \left[g_{p,i} - g_{q,i+\ell b} \right]^2 \qquad (26)$$

The latter equality in (26) makes use of the fact that the elements of $\underline{G}$ are all either zero or one, i.e., if x and y can only take on values zero and one, then $x+y-2xy = (x-y)^2$.

Each of the three summations in (26) is non-negative. Thus, in order for (26) to equal zero, each of these summations must itself be zero. Moreover, since the elements in each of the sums are non-negative, then the sum can be zero only if each element in each sum is zero. Thus, in conclusion, the

exponent $\alpha_p + \alpha_q - 2\beta_{pq}(\ell)$ can be zero only for those values of p, q, and ℓ for which (see Fig. 2)

$$g_{p,i} = 0 ; \quad i = (K-\ell)\,b + 1, (K-\ell)\,b + 2, \ldots, Kb$$

$$g_{q,i} = 0 ; \quad i = 1, 2, \ldots, \ell b$$

$$g_{p,i} = g_{q,i+\ell b} ; \quad i = 1, 2, \ldots, (K-\ell)\,b \tag{27}$$

This defines a class of convolutional codes whose significance will shortly become apparent. In the meantime it is sufficient to remark that if the code is such that (27) can be satisfied for any values of p, q, and ℓ (other than p = q and $\ell = 0$), then (25) is satisfied for all $\bar{a}$ (again including zero).

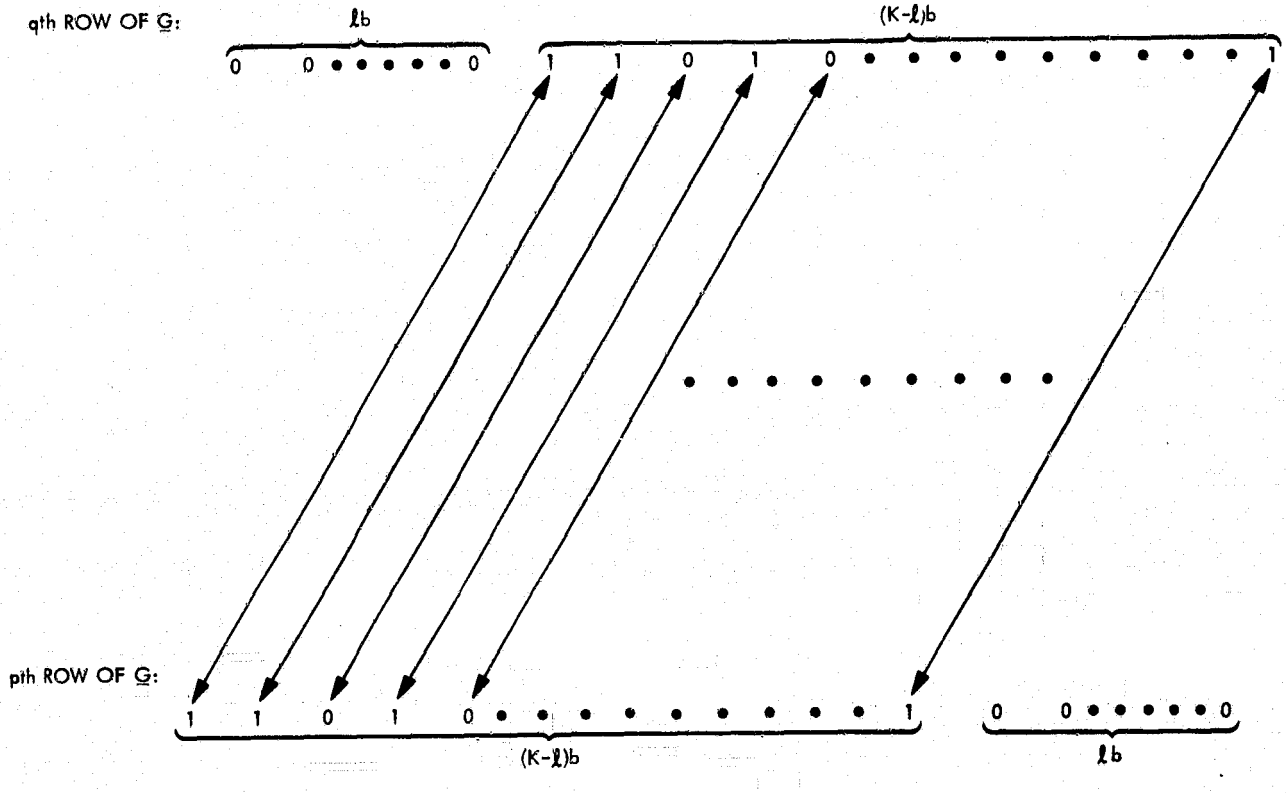

Figure 2. An Illustration of the Code Constraints of Equation (27)

Returning to (22), we further note that independent of the code, the exponent $\alpha_p + \alpha_q$ is never equal to zero. Thus, the term $(\bar{a})^{\alpha_p+\alpha_q}$ will be equal to one only when $\bar{a}$ is equal to one and will vanish when $\bar{a}$ is equal to zero (i.e., $p^* = 1/2$). This last statement is crucial to the results which now follow.

A. The Case of a Purely Random Data Input ($\bar{a} = 0$, $p^* = 1/2$)

Consider the special case of a random NRZ encoder input for which $p^* = 1/2$ and correspondingly, from (16), $\bar{a} = 0$. If the code is such that (27) is not satisfied for any combination of p, q, and ℓ (other than $p = q$ and $\ell = 0$), then from the previous discussion, the only nonzero terms in (22) will be the n terms corresponding to $p = q$ and $\ell = 0$ for which (25) applies. Thus, making use of (25) in (22) gives the simple result

$$S_X(f) = 1 \tag{28}$$

or

$$S_c(f) = T \left(\frac{\sin \pi fT}{\pi fT}\right)^2 \tag{29}$$

Furthermore, the discrete spectrum $S_d(f)$ of (23) vanishes. Thus, we reach the first important conclusion, namely, that for all codes which do not satisfy (27), a random NRZ data input results in a random NRZ data output scaled (expanded) in frequency by the reciprocal of the code rate, i.e., n/b. We define this class of codes as "uncorrelated convolutional codes."*

*Note, all rate 1/2, noncatastrophic convolutional codes are uncorrelated codes.

If, on the other hand, the code is such that (27) can be satisfied for at least one combination of p, q, ℓ (other than p = q and ℓ = 0), then $S_X(f)$ of (22) will be frequency dependent and the encoder output spectrum will not be merely a frequency scaled version of the input. In fact, letting $\{p, q, \ell\}$ denote the set of combinations of p, q, ℓ (other than p = q and ℓ = 0) for which (27) can be satisfied, then (22) simplifies to

$$S_X(f) = 1 + \frac{1}{n} \sum_{\{p,q,\ell\}} \sum \sum \epsilon_\ell \cos \left[2\pi (n\ell + q - p) fT\right] \tag{30}$$

Note that the discrete spectrum $S_d(f)$ of (23) still vanishes, since $\alpha_m \neq 0$; m = 1, 2, . . . , n; (i.e., independent of the code, the output symbol sequence cannot have a discrete spectrum for a purely random input).

We may now state the second important conclusion. Defining the class of codes which satisfy (27) (for at least one combination of p, q, ℓ other than p = q and ℓ = 0) as "correlated convolutional codes," then we observe that for such codes the encoder output spectrum will differ (in form) from the input spectrum.

At this point, it is instructive to give an example of a "correlated convolutional code" and calculate its output spectrum for a random NRZ input. Clearly, from Fig. 2, any code whose generator matrix is such that two or more rows are identical satisfies (27) with ℓ = 0 and is thus a correlated convolutional code. In a recent paper by Larsen (Ref. 2), short constraint length (up to and including K = 14) noncatastrophic codes with maximal free distance for rates 1/2, 1/3, and 1/4 were investigated and tabulated. Indeed, for rate 1/3 (n = 3), the tabulation includes only one correlated convolutional code which occurs for K = 3 (b = 1) and has the generator matrix

$$\underline{G} = \begin{bmatrix} 1 & 0 & 1 \\ 1 & 1 & 1 \\ 1 & 1 & 1 \end{bmatrix} \tag{31}$$

This code was first found by Odenwalder (Ref. 3). Since rows two and three of $\underline{G}$ are identical, we must evaluate (30) for the two combinations p = 2, q = 3, ℓ = 0, and p = 3, q = 3, ℓ = 0. Doing so results in the simple result

$$S_X(f) = 1 + \frac{2}{3}\cos 2\pi fT \tag{32}$$

Multiplying $S_X(f)$ of (32) by $S_p(f)$ of (24) gives the encoder output spectrum $S_c(f)$ which is plotted in Fig. 3.

For rate 1/4 (n = 4), the tabulation in Ref. 2 reveals three correlated convolutional codes corresponding to constraint lengths K = 3, 4, and 7. For the K = 3 code, for example, the free distance is ten (this is the maximum achievable), and the generator matrix is given by

$$\underline{G} = \begin{bmatrix} 1 & 0 & 1 \\ 1 & 1 & 1 \\ 1 & 1 & 1 \\ 1 & 1 & 1 \end{bmatrix} \tag{33}$$

which is identical to (31) except for the addition of another identical row. Thus, following the same procedure as above, we find that

$$S_X(f) = 1 + \frac{1}{2}\left[2\cos 2\pi fT + \cos 4\pi fT\right] \tag{34}$$

which together with (24) gives the output encoder spectrum illustrated in Fig. 4.

Code Generator Matrix

1 0 1
1 1 1
1 1 1

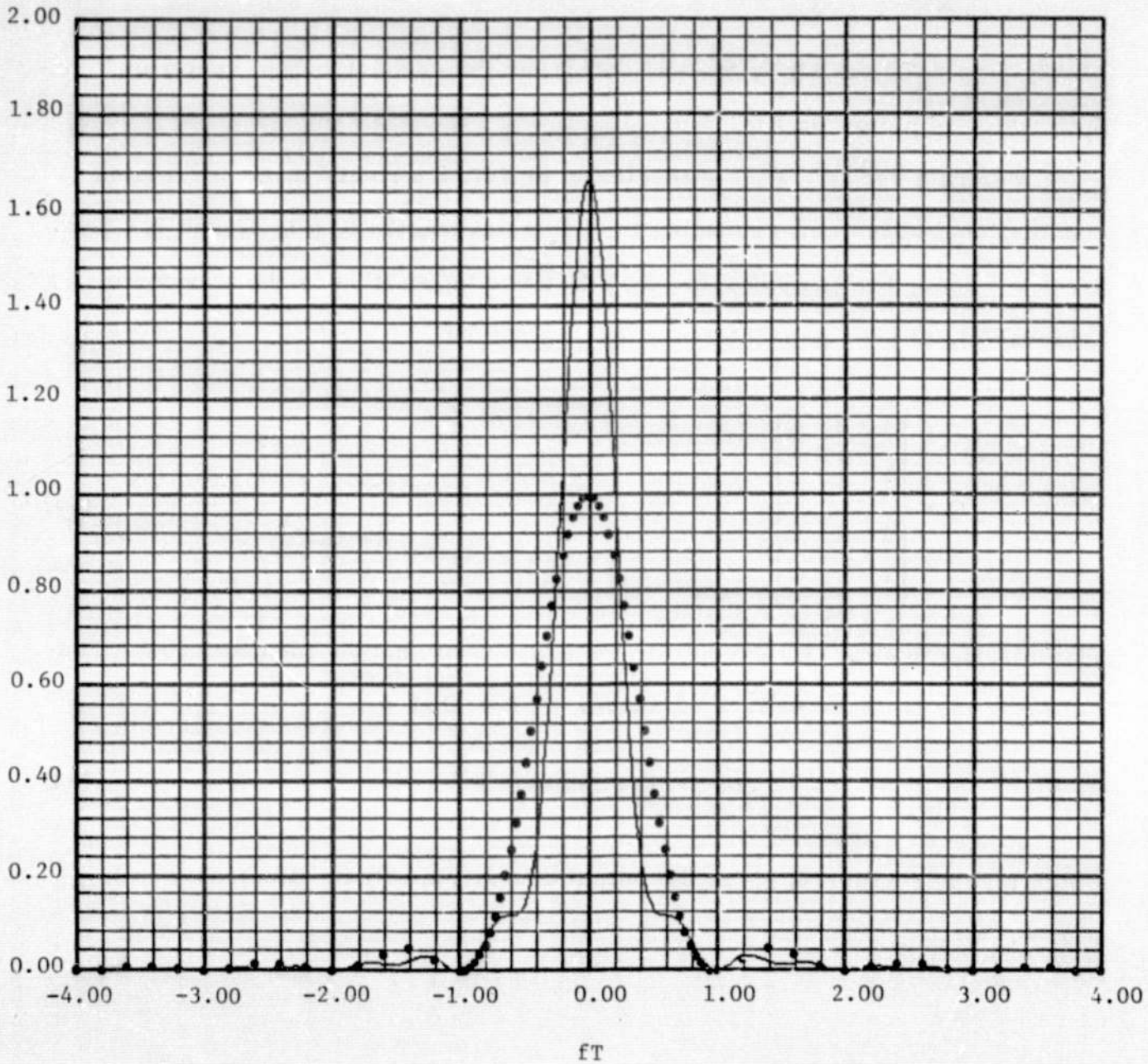

Figure 3. Spectrum for Best Rate 1/3; Constraint Length 3 Convolutional Code; Dotted Curve is Spectrum of NRZ

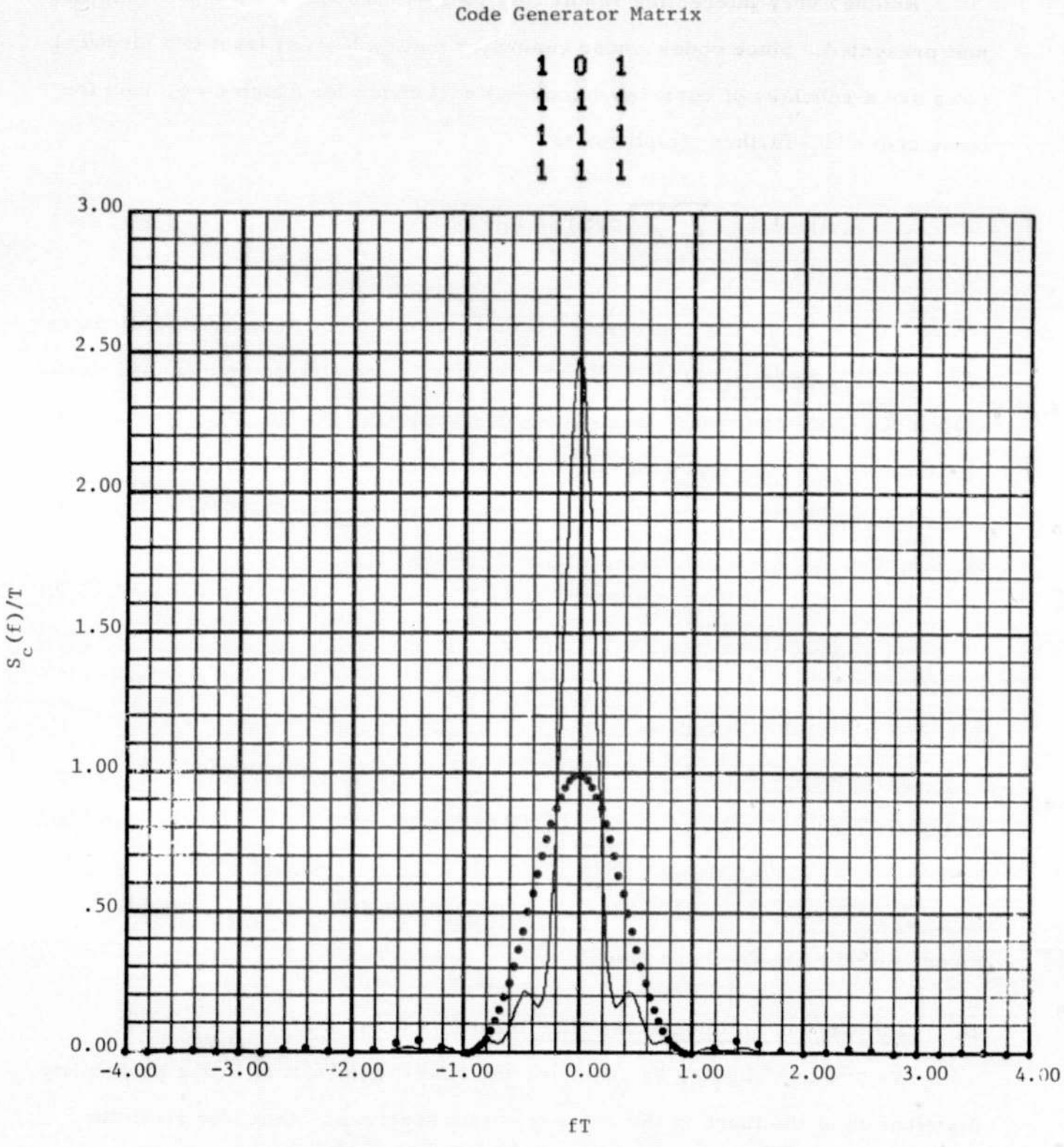

Figure 4. Spectrum for Best Rate 1/4; Constraint Length 3 Convolutional Code; Dotted Curve is Spectrum of NRZ

Another very interesting result may be gleaned from the simple examples just presented. Since codes whose generator matrix have at least two identical rows are a subclass of correlated convolutional codes for which $\ell = 0$, then for these codes (30) further simplifies to

$$S_X(f) = 1 + \frac{1}{n} \sum\sum_{\{p,q\}} \cos\left[2\pi\,(q - p)\,fT\right] \tag{35}$$

where the set $\{p, q\}$ now represents all pairs of integers corresponding to pairs of identical rows in $\underline{G}$. Since (34) only depends on the difference q-p, and small values of q-p correspond to less oscillatory behavior of $S_X(f)$, then it is clearly desirable from a spectral concentration standpoint to have the identical rows packed close together. For example, if the bottom row of $\underline{G}$ in (31) is moved to the top, then p - q = 2 and the spectrum $S_X(f)$ becomes

$$S_X(f) = 1 + \frac{2}{3} \cos 4\pi fT \tag{36}$$

which is illustrated in Fig. 5.

The important point to realize from the above is that permuting the rows of the generator matrix of a convolutional code can be used to change the encoder output spectrum without any effect on the bit error probability performance of the code. Further examples and extensions of this statement will be given along with the results that follow.

B. The Case of an Unbalanced NRZ Input ($\bar{a} \neq 0$, $p^* \neq 1/2$)

We now investigate, by example, the effect of unbalance in the probability distribution of the input on the encoder output spectrum. Consider first the

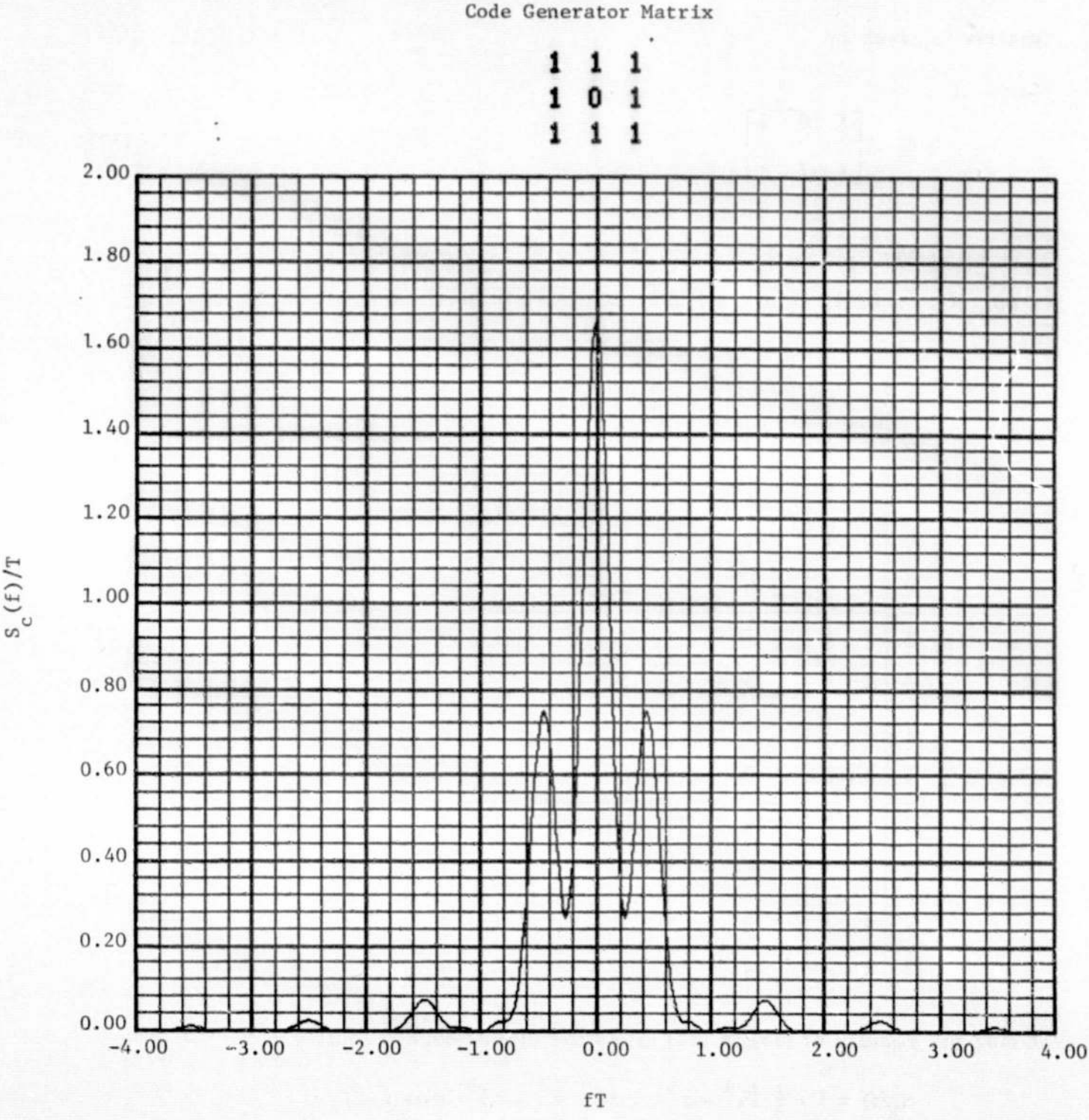

Figure 5. Spectrum for Best Rate 1/3, Constraint Length 3 Convolutional Code

simple case of the optimum rate 1/2, constraint length 3 code whose generator matrix is given by

$$\underline{G} = \begin{bmatrix} 1 & 0 & 1 \\ 1 & 1 & 1 \end{bmatrix} \tag{37}$$

For this code $\alpha_1 = 2$, $\alpha_2 = 3$ and the sets of exponents $\alpha_p + \alpha_q$ and $\alpha_p + \alpha_q - 2\beta_{pq}(\ell)$; $\ell = 0, 1, 2$; $p, q = 1, 2$ is tabulated below:

ℓ	p	q	$2\ell + q - p$	$\alpha_p + \alpha_q$	$\alpha_p + \alpha_q - 2\beta_{pq}(\ell)$
0	1	1	0	4	0
0	1	2	1	5	1
0	2	1	-1	5	1
0	2	2	0	6	0
1	1	1	2	4	4
1	1	2	3	5	3
1	2	1	1	5	3
1	2	2	2	6	2
2	1	1	4	4	2
2	1	2	5	5	3
2	2	1	3	5	3
2	2	2	4	6	4

(38)

Using the results of (38) in (22) gives the closed form result

$$\begin{aligned} S_X(f) = 1 - \frac{1}{2}\left(\bar{a}^4 - \bar{a}^6\right) + \left(\bar{a} + \bar{a}^3 - 2\bar{a}^5\right) \cos 2\pi fT \\ + \left(\bar{a}^2 - \bar{a}^6\right) \cos 4\pi fT + 2\left(\bar{a}^3 - \bar{a}^5\right) \cos 6\pi fT \\ + \left(\bar{a}^2 - \bar{a}^6\right) \cos 8\pi fT + \left(\bar{a}^3 - \bar{a}^5\right) \cos 10\pi fT \end{aligned} \tag{39}$$

Since this code is an uncorrelated convolutional code, (30) should reduce to $S_X(f) = 1$ for $\bar{a} = 0$ which indeed it does.

Figure 6 is an illustration of the continuous component of the encoder output spectrum $S_c(f)$ [obtained by multiplying $S_X(f)$ of (39) by $S_p(f)$ of (24)] for various values of $p^* = (1 - \bar{a})/2$. We observe that the spectrum becomes more and more concentrated as p^* decreases. The continuous component of the input spectrum, on the other hand, remains unaltered in shape as p^* is varied. In particular, for a unit power unbalanced NRZ input, the power spectral density is given by (Ref. 4)

$$S(f) = (1 - 2p^*)^2 \, \delta(f) + 4p^* (1 - p^*) \, T_b \left(\frac{\sin \pi f T_b}{\pi f T_b} \right)^2 \tag{40}$$

where T_b is the input bit time.

The discrete component of the output spectrum $S_d(f)$ is easily found from (23) to be

$$S_d(f) = \left(\bar{a}^3 - \bar{a}^2 \right)^2 \sum_{k=1,3,5\ldots}^{\infty} \left(\frac{1}{\pi k} \right)^2 \delta \left(f - \frac{k}{2T} \right) \tag{41}$$

As a second example, consider the optimum rate 1/2, constraint length 7 code whose generator matrix is given by (Ref. 3, 5)

$$\underline{G} = \begin{bmatrix} 1 & 1 & 1 & 1 & 0 & 0 & 1 \\ 1 & 0 & 1 & 1 & 0 & 1 & 1 \end{bmatrix} \tag{42}$$

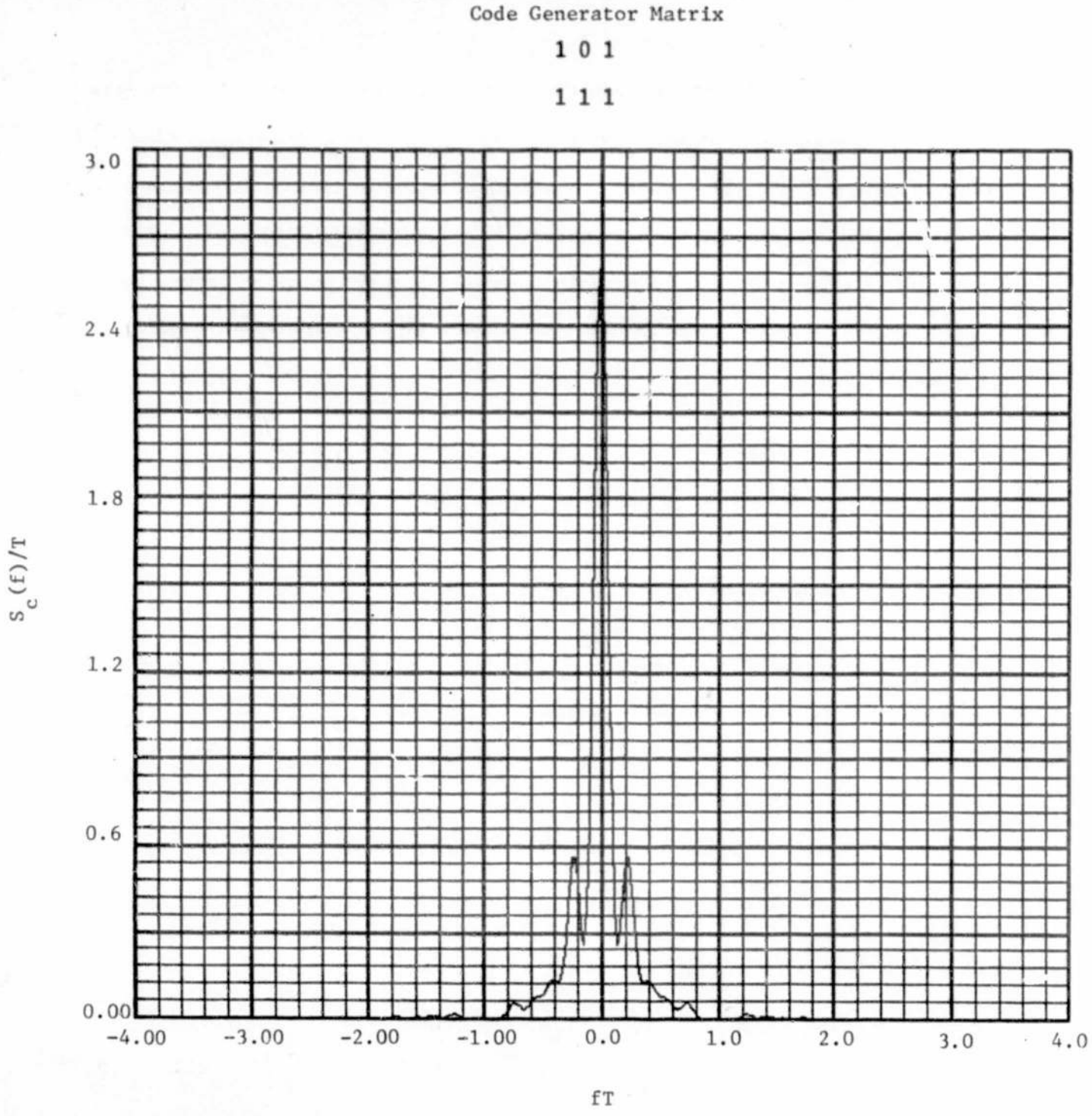

Figure 6a. Spectrum for Best Rate 1/2, Constraint Length 3 Convolutional Code; $p^* = 0.1$

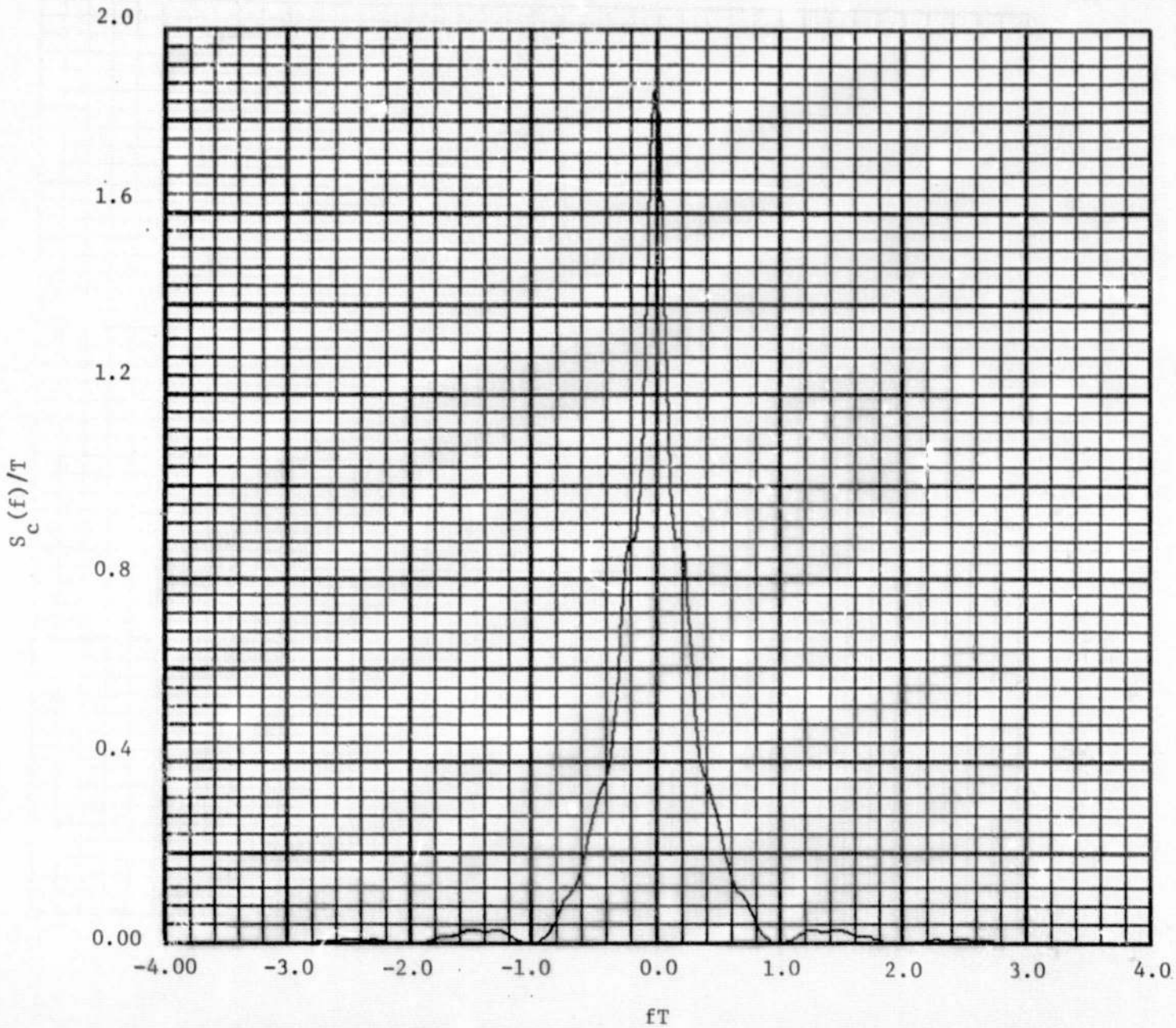

Figure 6b. Spectrum for Best Rate 1/2, Constraint Length 3 Convolutional Code; $p^* = 0.3$

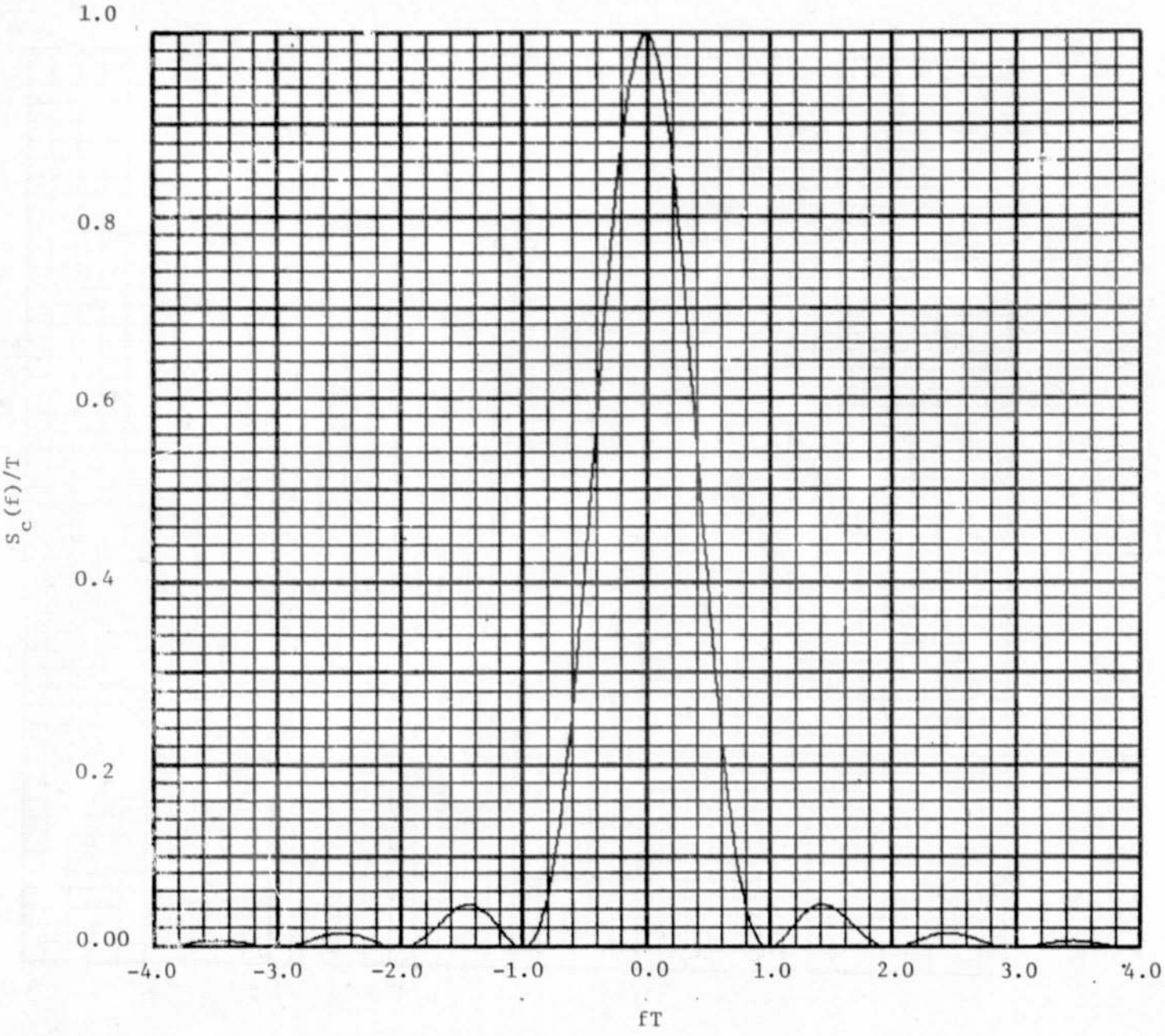

Figure 6c. Spectrum for Best Rate 1/2, Constraint Length 3 Convolutional Code; p* = 0.5

Since for this code $\alpha_1 = \alpha_2 = 5$, then because of this balance in the number of ones in both rows of the matrix, we immediately see from (23) that the encoder output will only contain a discrete spectrum at f = 0, i.e., $S_d(f) = (\bar{a})^5 \delta(f)$*. The continuous component of the output spectrum can once again be obtained from (22) where $S_X(f)$ is now given by

$$S_X(f) = 1 - \bar{a}^{10} + \left(\bar{a}^2 + \bar{a}^6 - \bar{a}^{10}\right) \cos 2\pi fT + \left(\bar{a}^4 + \bar{a}^6 - 2\bar{a}^{10}\right) \cos 4\pi fT$$
$$+ 2\left(\bar{a}^4 - \bar{a}^{10}\right) \cos 6\pi fT + 2\left(\bar{a}^6 - \bar{a}^{10}\right) \left[\cos 8\pi fT + \cos 14\pi fT\right]$$
$$+ \left(\bar{a}^4 + \bar{a}^8 - 2\bar{a}^{10}\right) \cos 10\pi fT + \left(\bar{a}^4 + \bar{a}^6 - 2\bar{a}^{10}\right) \cos 12\pi fT$$
$$+ 2\left(\bar{a}^8 - \bar{a}^{10}\right) \left[\cos 16\pi fT + \cos 20\pi fT + \frac{1}{2} \cos 22\pi fT\right.$$
$$\left. + \cos 24\pi fT + \frac{1}{2} \cos 26\pi fT\right] + \left(\bar{a}^6 + \bar{a}^8 - 2\bar{a}^{10}\right) \cos 18\pi fT \tag{43}$$

Figure 7 is an illustration of the corresponding continuous spectrum $S_c(f)$ for several values of $p^* = (1 - \bar{a})/2$. As before, we observe that the output encoder spectrum narrows as p^* is decreased.

An interesting thing now happens if, for example, we reverse the direction of the sampler (commutator) at the output of the encoder. This is equivalent to interchanging the two rows in the $\underline{G}$ matrix of (42). Since the two rows still contain the identical number of ones, i.e., $\alpha_1 = \alpha_2 = 5$, then the discrete

*For any code with $\alpha_1 = \alpha_2 = \ldots \alpha_m \triangleq \alpha$, Eq. (23) will simplify to $S_d(f) = (\bar{a})^\alpha \delta(f)$.

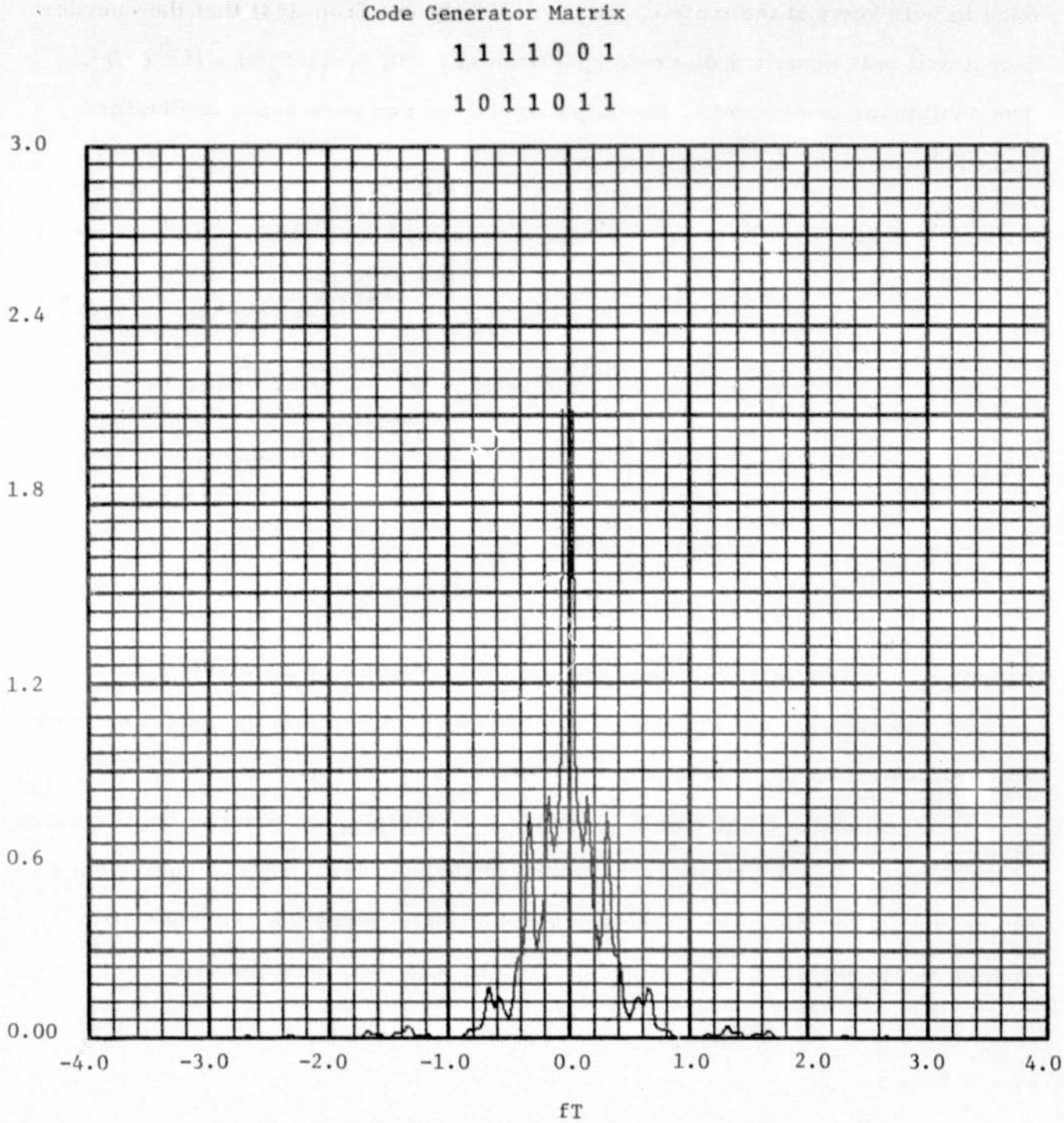

Figure 7a. Spectrum for Best Rate 1/2, Constraint Length 7 Convolutional Code; $p^* = 0.1$

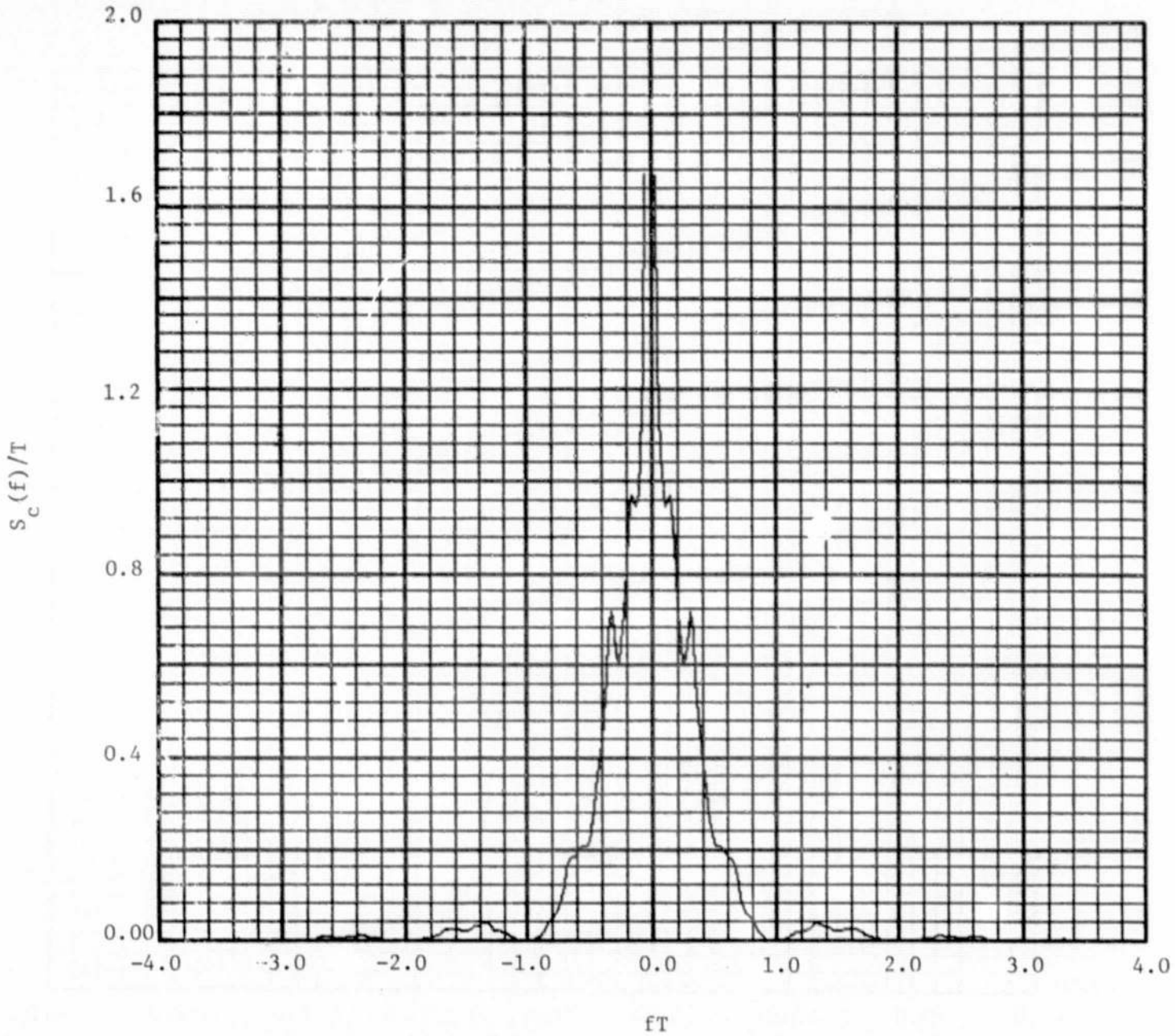

Figure 7b. Spectrum for Best Rate 1/2, Constraint Length 7 Convolutional Code; $p^* = 0.2$

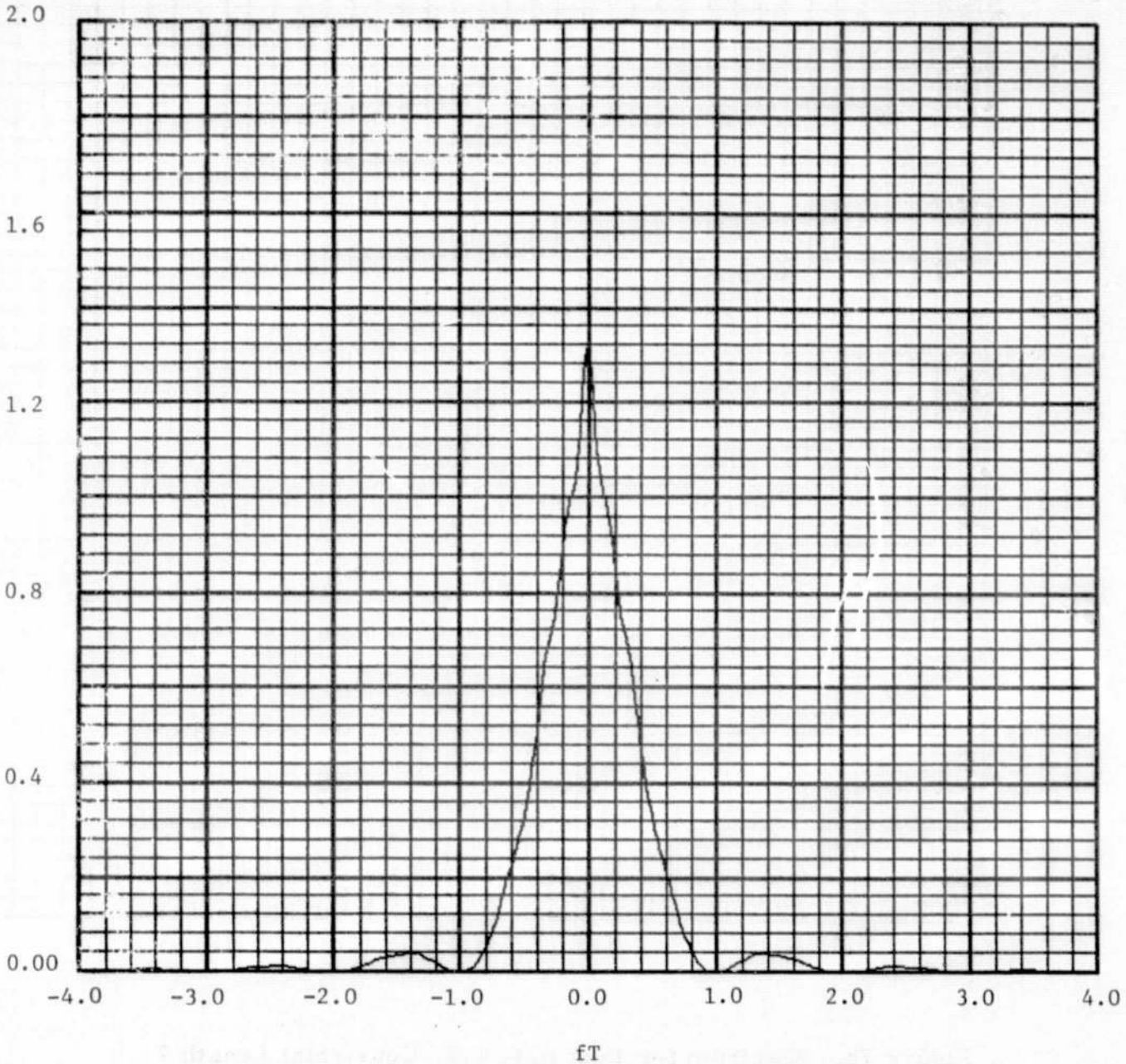

Figure 7c. Spectrum for Best Rate 1/2, Constraint Length 7 Convolutional Code; p* = 0.3

spectral component of the encoder output is unchanged. However, the continuous component of the encoder output spectrum is not characterized by (43) but rather by

$$
\begin{aligned}
S_X(f) = {} & 1 - \bar{a}^{10} + \left(\bar{a}^2 + \bar{a}^4 - 2\bar{a}^{10}\right) \cos 2\pi fT \\
& + \left(\bar{a}^4 + \bar{a}^6 - 2\bar{a}^{10}\right) \left[\cos 4\pi fT + \cos 10\pi fT + \cos 12\pi fT\right] \\
& + \left(\bar{a}^6 + \bar{a}^8 - 2\bar{a}^{10}\right) \left[\cos 6\pi fT + \cos 22\pi fT\right] \\
& + 2\left(\bar{a}^6 - \bar{a}^{10}\right) \left[\cos 8\pi fT + \tfrac{1}{2} \cos 18\pi fT\right] \\
& + \left(\bar{a}^4 + \bar{a}^8 - 2\bar{a}^{10}\right) \cos 14\pi fT \\
& + 2\left(\bar{a}^8 - \bar{a}^{10}\right) \left[\cos 16\pi fT + \cos 20\pi fT \right. \\
& \left. + \cos 24\pi fT + \tfrac{1}{2} \cos 26\pi fT\right]
\end{aligned}
\tag{44}
$$

The corresponding continuous spectrum component $S_c(f)$ is illustrated in Fig. 8 for the same values of p* as in Fig. 7. Comparing these two figures, it is difficult to draw any decisive conclusions regarding their relative spectral width other than to note that the two spectra are quite different.

We conclude this section by noting that reversing the sampler for the rate 1/2, constraint length 3 code characterized by $\underline{G}$ of (37) would not alter the spectrum. The reason for this conclusion is that the two rows of $\underline{G}$ have even symmetry about their midpoint (i.e., the elements in column 2). This is not true for the generator matrix of (42) and it is indeed this lack of even symmetry which makes the encoder output spectrum dependent on the sampler direction.

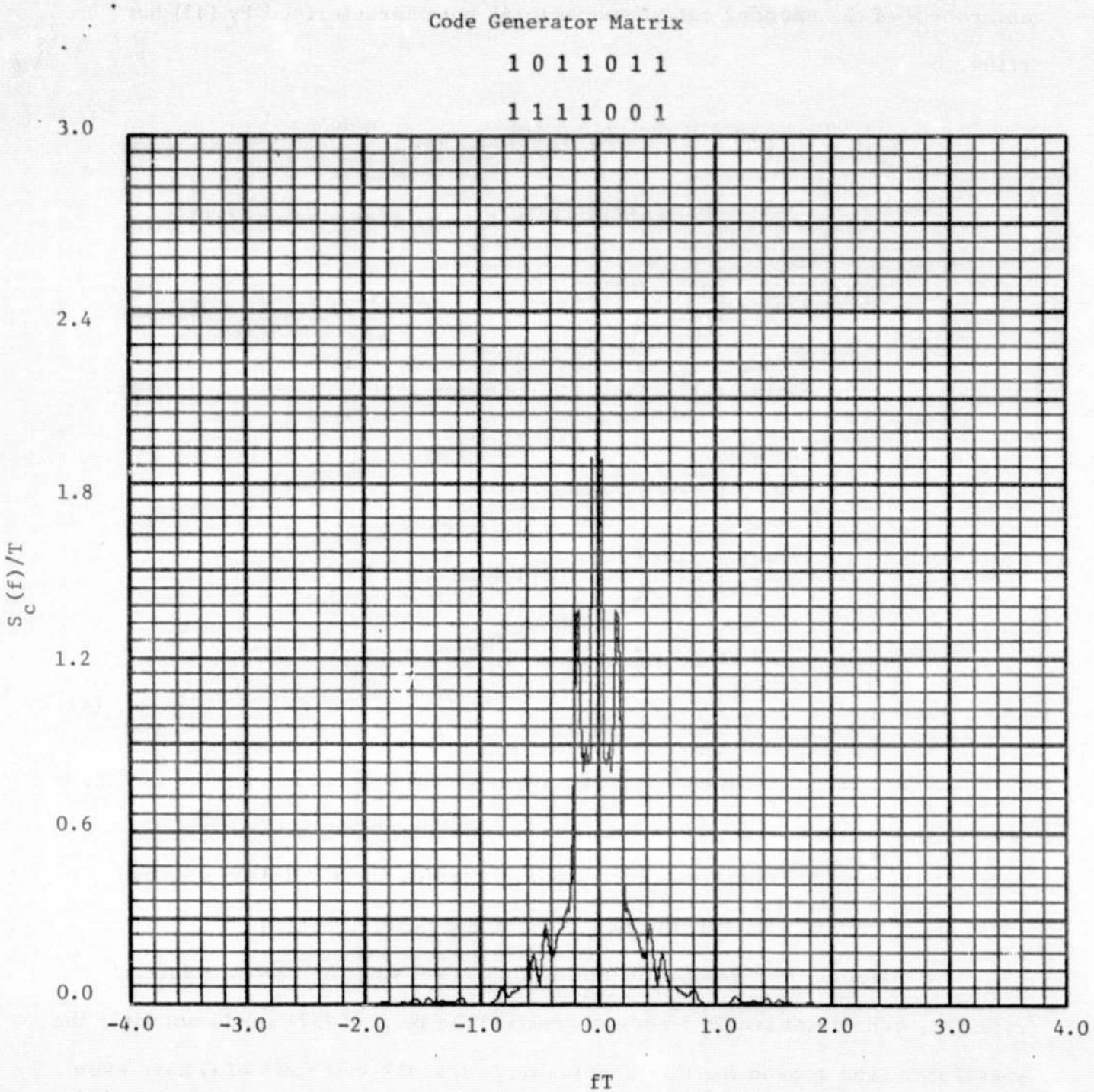

Figure 8a. Spectrum for Best Rate 1/2, Constraint Length 7 Convolutional Code; Sampler Reversed; $p^* = 0.1$

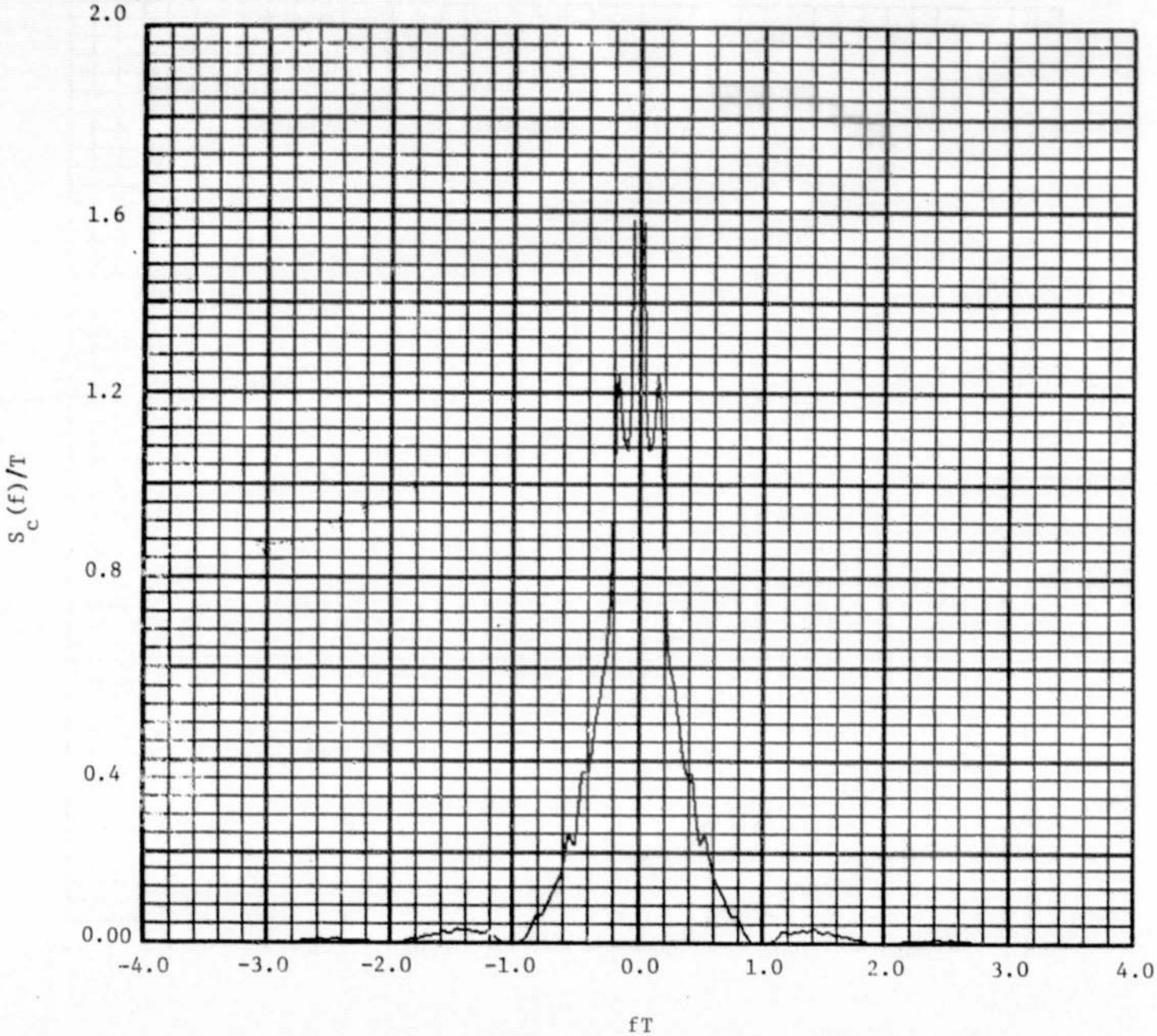

Figure 8b. Spectrum for Best Rate 1/2, Constraint Length 7 Convolutional Code; Sampler Reversed; $p^* = 0.2$

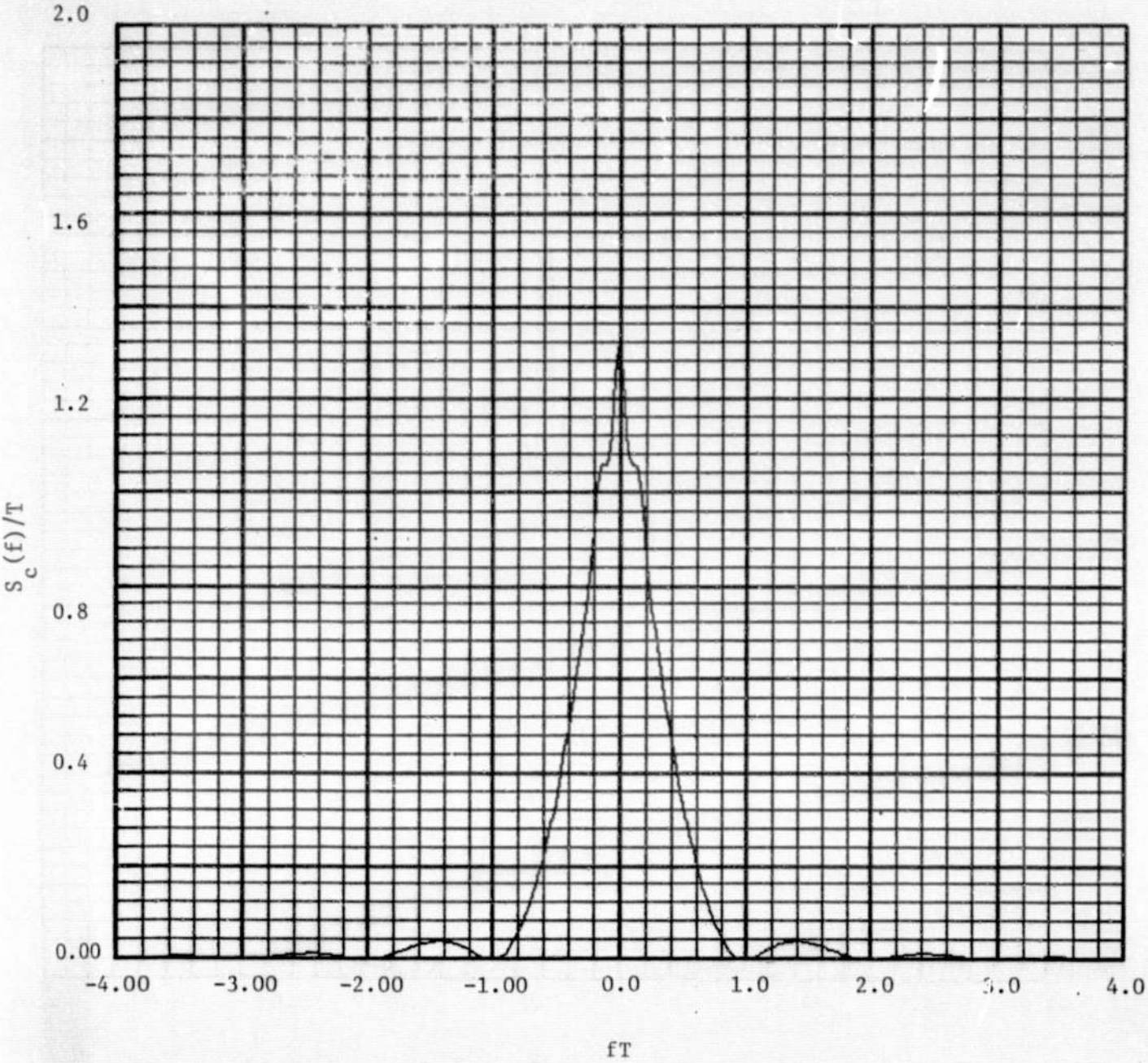

Figure 8c. Spectrum for Best Rate 1/2, Constraint Length 7 Convolutional Code; Sampler Reversed; $p^* = 0.3$

V. Encoder Output Spectrum for First Order Markov Input

For the first order Markov case, we first transform the information bit sequence $\{a_j\}$ into a transition sequence $\{t_j\}$, where $t_j = a_j\, a_{j-1}$; $j = 1, 2, \ldots$ The sequence $\{t_j\}$ is a stationary sequence of independent random variables with

$$\Pr\{t_j = -1\} = 1 - \Pr\{t_j = 1\} = p_t$$

$$E\{t_j\} = 1 - 2p_t \triangleq \bar{t} \tag{45}$$

where p_t is the transition density. For any ℓ and $n \geq 1$ we have

$$a_{\ell-n} = a_\ell \prod_{i=1}^{n} t_{\ell-i+1} \tag{46a}$$

$$a_{\ell+n} = a_\ell \prod_{i=1}^{n} t_{\ell+i} \tag{46b}$$

Recalling from (1) that for $m = 0$,

$$X_p = \prod_{i=1}^{Kb} \left(a_{b-i}\right)^{g_{p,i}} \tag{47}$$

then, substituting (46a) with $\ell = b - 1$ into (47) results after simplification in

$$X_p = \left(a_{b-1}\right)^{\alpha_{p,1}} \prod_{i=1}^{Kb-1} \left(t_{b-i}\right)^{\alpha_{p,i+1}} \tag{48}$$

where

$$\alpha_{p,i} = \sum_{j=i}^{Kb} g_{p,j} \tag{49}$$

Note that $\alpha_{p,1} = \alpha_p$ of (19). Since the elements of the sequences $\{a_j\}$ and $\{t_j\}$ can only take on values ± 1, then the algebraic sum of (49) can be replaced by a modulo 2 sum. Defining

$$h_{p,i} = \sum_{j=i}^{Kb} g_{p,j} \tag{50}$$

then (48) can be equivalently written as

$$X_p = \left(a_{b-1}\right)^{h_{p,1}} \prod_{i=1}^{Kb-1} \left(t_{b-i}\right)^{h_{p,i+1}} \tag{51}$$

where $\sum$ denotes modulo 2 summation. Note that (50) defines a "modified generator matrix" $\underline{H}$ with (0, 1) elements which is uniquely related to the connection matrix $\underline{G}$. In fact, each element in $\underline{H}$ is merely the modulo 2 sum of the corresponding element in $\underline{G}$ with those in the remainder of that row. Using (46b) we can similarly write

$$X_{n\ell+q} = \left(a_{b-1}\right)^{h_{q,1}} \prod_{j=1}^{\ell b} \left(t_{b-1+j}\right)^{h_{q,1}} \prod_{i=1}^{Kb-1} t_{(\ell+1)b-i} \tag{52}$$

To evaluate the encoder output spectrum factor $S_X(f)$ of (12), we require the covariance of X_p of (51) and $X_{n\ell+q}$ of (52). To compute this covariance we first define

$$\rho_p \triangleq \sum_{i=2}^{Kb} h_{p,i} \tag{53}$$

Then, from (51),

$$\overline{X}_p = (1 - h_{p,1})\,(\bar{t})^{\rho_p} \tag{54}$$

and

$$\overline{X_p\, X_{n\ell+q}} = \left[1 - \left(h_{p,1} \oplus h_{q,1}\right)\right](\bar{t})^{\gamma_{p,q}(\ell)} \tag{55}$$

where for $1 \le \ell \le K-1$

$$\gamma_{p,q}(\ell) = \sum_{i=2}^{\ell b+1} \left(h_{q,1} \oplus h_{q,i}\right) + \sum_{i=\ell b+2}^{Kb} \left(h_{q,i+1} \oplus h_{p,i-\ell b+1}\right) + \sum_{i=(K-\ell)b+1}^{Kb} h_{p,i} \tag{56}$$

The result in (56) can be simplified by noting that for x and y both (0, 1) variables,

$$x \oplus y = x + y - 2xy \tag{57}$$

Thus,

$$\gamma_{p,q}(\ell) = \rho_p + \rho_q - 2\xi_{p,q}(\ell) \; ; \qquad 1 \le \ell \le K - 1 \tag{58}$$

where

$$\xi_{p,q}(\ell) = \sum_{i=2}^{(K-\ell)b} h_{p,i}\, h_{q,i+\ell b} - \frac{1}{2} h_{q,1} \left(2 + \ell b - 2 \sum_{i=1}^{\ell b} h_{q,i} \right) \tag{59}$$

The relation in (58) can also be shown to hold for $\ell = 0$ and $\ell \ge K$ in which case

$$\xi_{pq}(\ell) = \begin{cases} \sum_{i=2}^{Kb} h_{p,i}\, h_{q,i} \; ; & \ell = 0 \\ \left(\rho_q - \frac{1}{2} \ell b \right) h_{q,1} \; ; & \ell \ge K \end{cases} \tag{60}$$

Thus, using (54), (55), (57) and (58) and recognizing analogous symmetry properties for $\ell < 0$ as used in obtaining (20), the desired covariance is given by

$$\operatorname{cov}\left(X_p\, X_{n\ell+q} \right) = \begin{cases} \left[1 - h_{p,1} - h_{q,1} + 2h_{p,1}\, h_{q,1} \right] (\bar{t})^{\rho_p + \rho_q - 2\xi_{p,q}(\ell)} \\ \qquad - \left(1 - h_{p,1} \right) (\bar{t})^{\rho_p + \rho_q} \; ; & \ell \ge 0 \\ \left[1 - h_{p,1} - h_{q,1} + 2h_{p,1}\, h_{q,1} \right] (\bar{t})^{\rho_q + \rho_p - 2\xi_{q,p}(-\ell)} \\ \qquad - \left(1 - h_{p,1} \right) (\bar{t})^{\rho_q + \rho_p} \; ; & \ell \le 0 \end{cases} \tag{61}$$

Note the similarity in form between (20) and (61). The prinicpal difference between the two is that (20) corresponds to a cyclostationary process with memory equal to K-1 whereas the memory of the process characterized by (61) is infinite.

Finally, substituting (61) into (12) and performing considerable simplification gives the desired result, analogous to (22), namely,

$$S_X(f) = \frac{1}{n}\sum_{p=1}^{n}\sum_{q=1}^{n}\left(1 - h_{p,1} - h_{q,1} + 2h_{p,1}\,h_{q,1}\right)\sum_{\ell=0}^{K-1}\epsilon_\ell$$

$$\times\left[(\bar{t})^{\rho_p + \rho_q - 2\xi_{p,q}(\ell)} - \left(1 - h_{q,1}\right)(\bar{t})^{\rho_p + \rho_q}\right]$$

$$\times\cos\left[2\pi\,(n\ell + q - p)\,fT\right]$$

$$+\frac{2}{n}\sum_{p=1}^{n}\sum_{q=1}^{n} h_{p,1}\,h_{q,1}\,(\bar{t})^{\rho_p + \rho_q + Kb}$$

$$\times\frac{\cos\left[2\pi\,(nK + q - p)\,fT\right] - \bar{t}^{b}\cos\left[2\pi\,(n\,(K-1) + q - p)\,fT\right]}{1 - 2\,\bar{t}^{b}\cos 2\pi nfT + \bar{t}^{2b}}$$

$$S_c(f) = T\left(\frac{\sin \pi fT}{\pi fT}\right)^2 S_X(f) \qquad (62)$$

The discrete spectrum $S_d(f)$ at the encoder output is obtained by substituting $\overline{X}_p$ of (54) into (15). Thus,

$$S_d(f) = \frac{1}{n^2} \sum_{k=-\infty}^{\infty} \left(\frac{\sin \frac{\pi k}{n}}{\frac{\pi k}{n}} \right)^2 \left\{ \left[\sum_{m=1}^{n} \left(1 - h_{m,1}\right) \bar{t}^{\rho m} \cos \left(\frac{2\pi mk}{n} \right) \right]^2 \right.$$

$$\left. + \left[\sum_{m=1}^{n} \left(1 - h_{m,1}\right) \bar{t}^{\rho m} \sin \left(\frac{2\pi mk}{n} \right) \right]^2 \right\} \delta \left(f - \frac{k}{n\bar{T}} \right) \tag{63}$$

Note that a discrete spectrum can potentially exist at the encoder output despite the fact that the encoder input has only a continuous spectrum. In fact, for a first order Markov source as the encoder input, its spectrum is given by (Appendix A)

$$S(f) = \left(\frac{1 - \bar{t}^2}{1 + \bar{t}^2 - 2\bar{t} \cos 2\pi f T_b} \right) T_b \left(\frac{\sin \pi f T_b}{\pi f T_b} \right)^2 \tag{64}$$

where T_b is again the input bit time (see Fig. 9). Note that if the code is <u>transparent</u>, i.e., each row of $\underline{G}$ has an odd number of ones, then from (50)

$$h_{p,i} = 1 \; ; \qquad p = 1, 2, \ldots, n \tag{65}$$

which when substituted in (63) results in $S_d(f) = 0$.

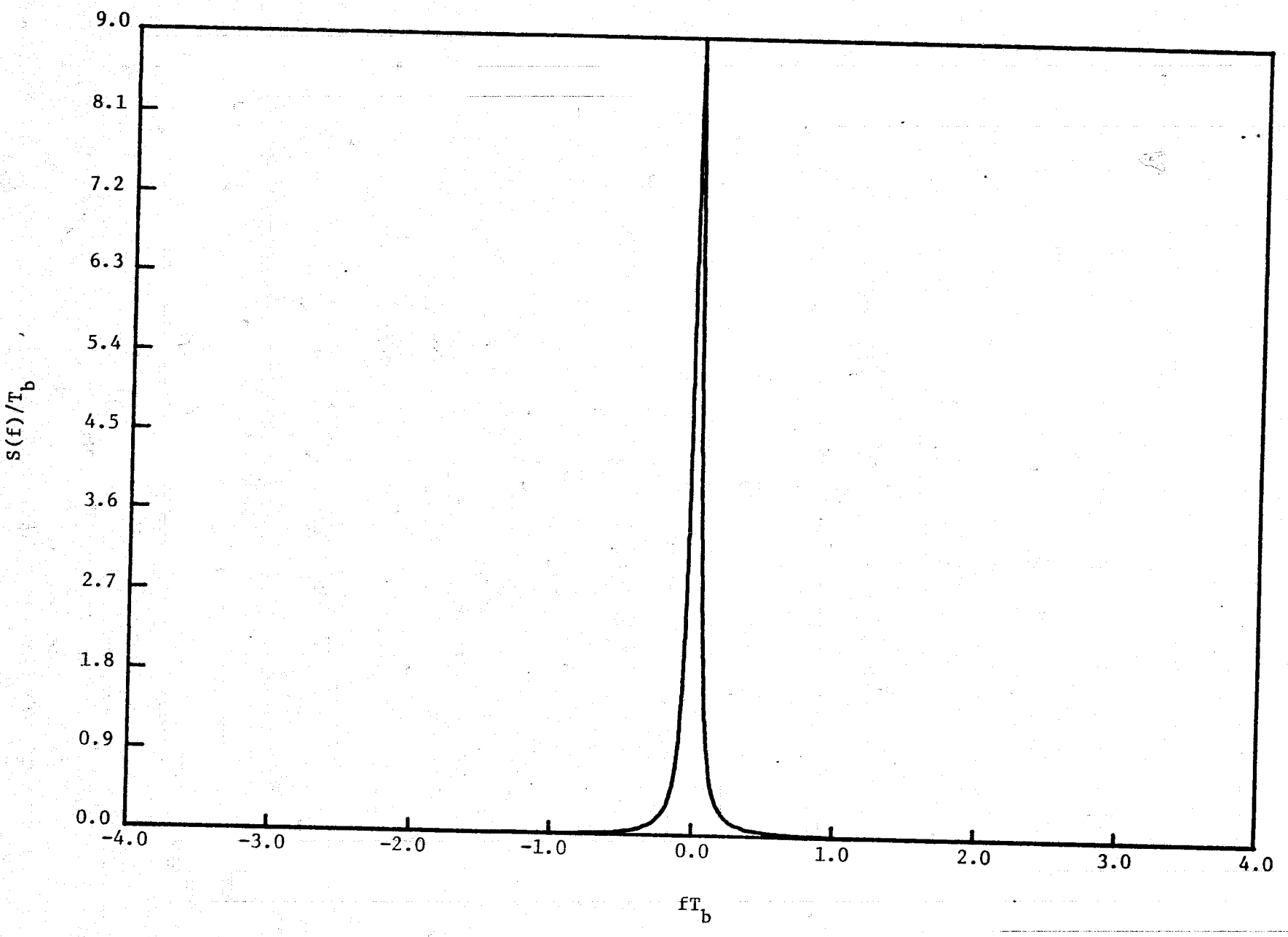

Figure 9a. Power Spectrum of First Order Markov Source; $p_t = 0.1$

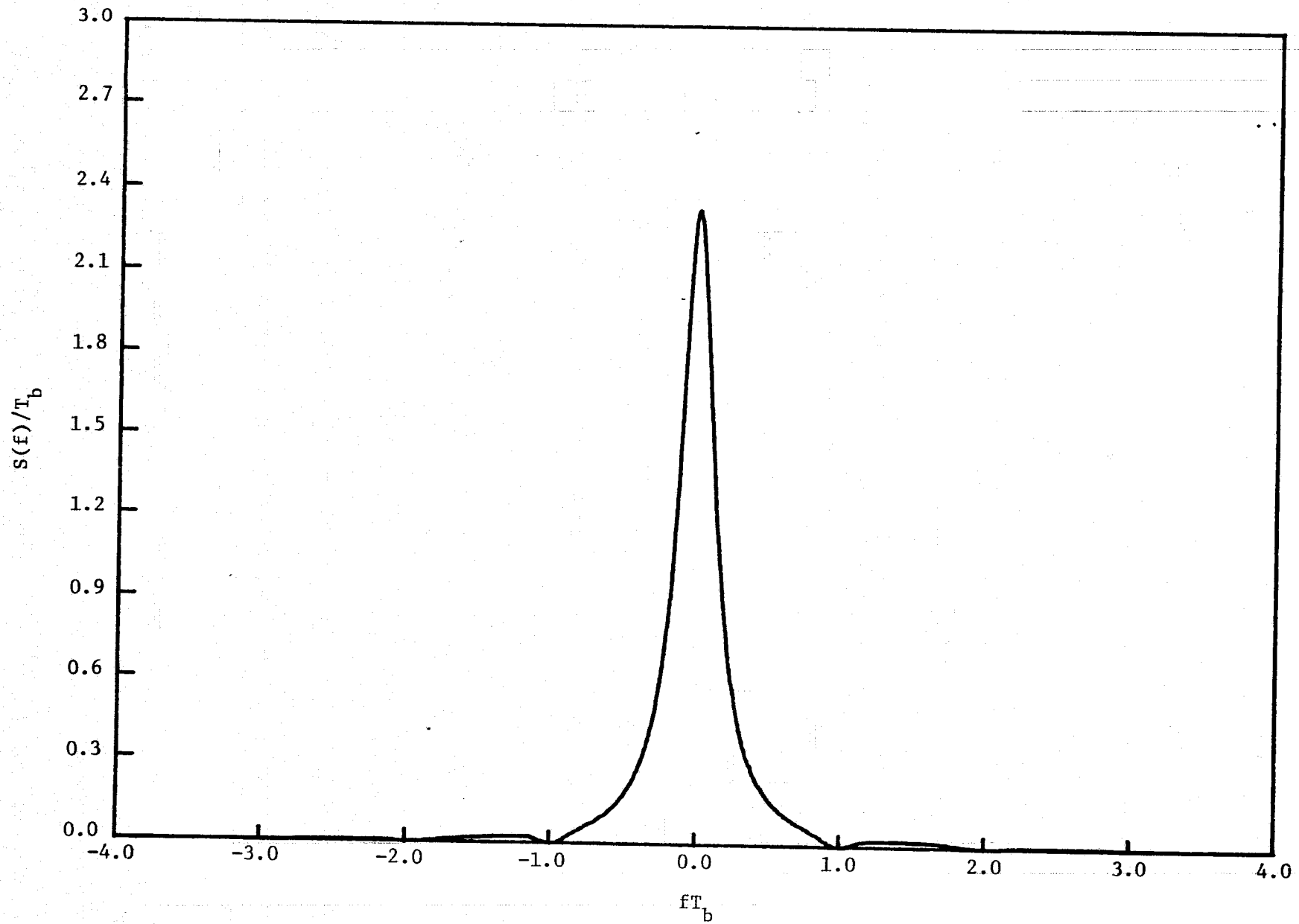

Figure 9b. Power Spectrum of First Order Markov Source; $p_t = 0.3$

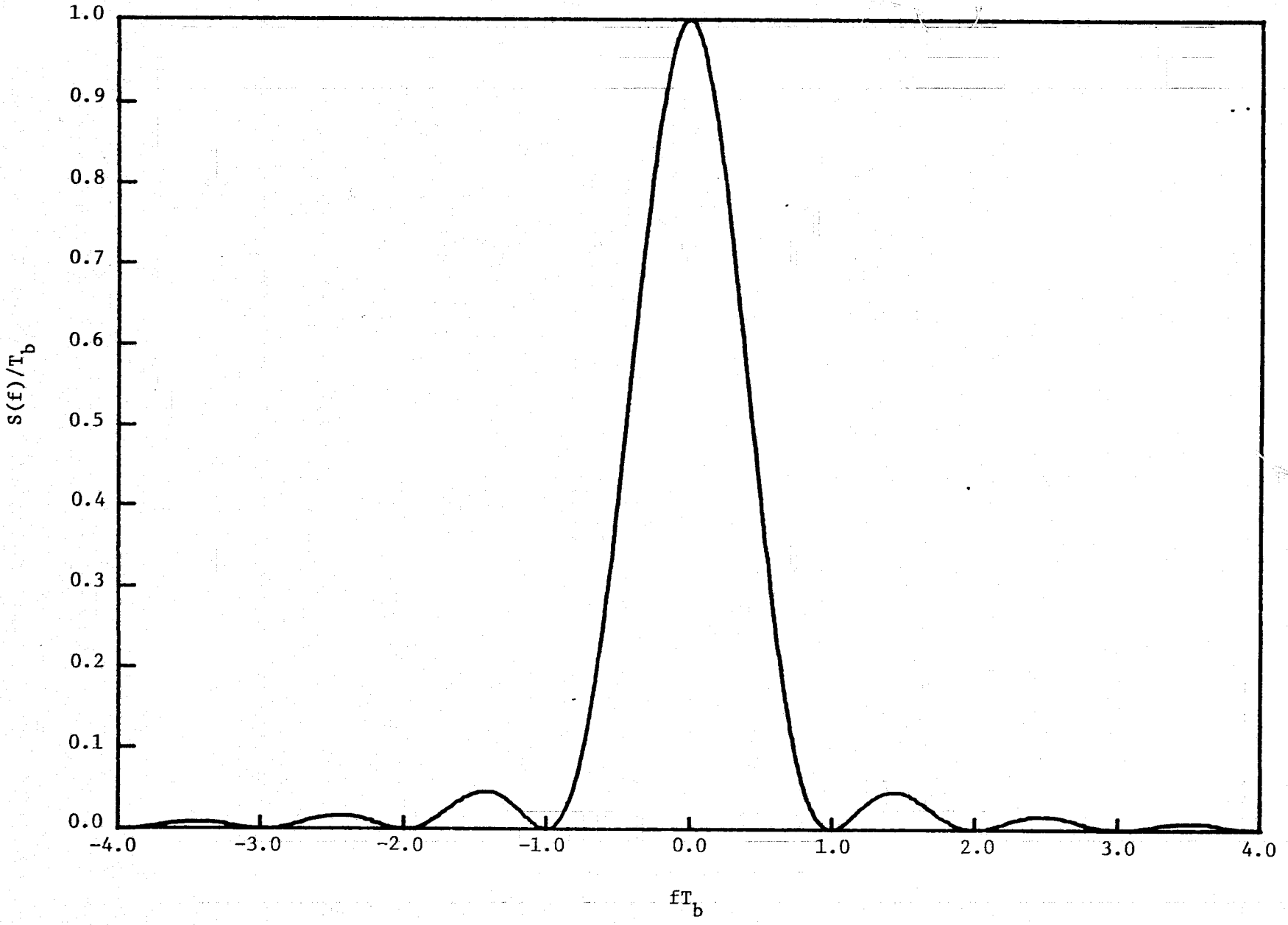

Figure 9c. Power Spectrum of First Order Markov Source; $p_t = 0.5$

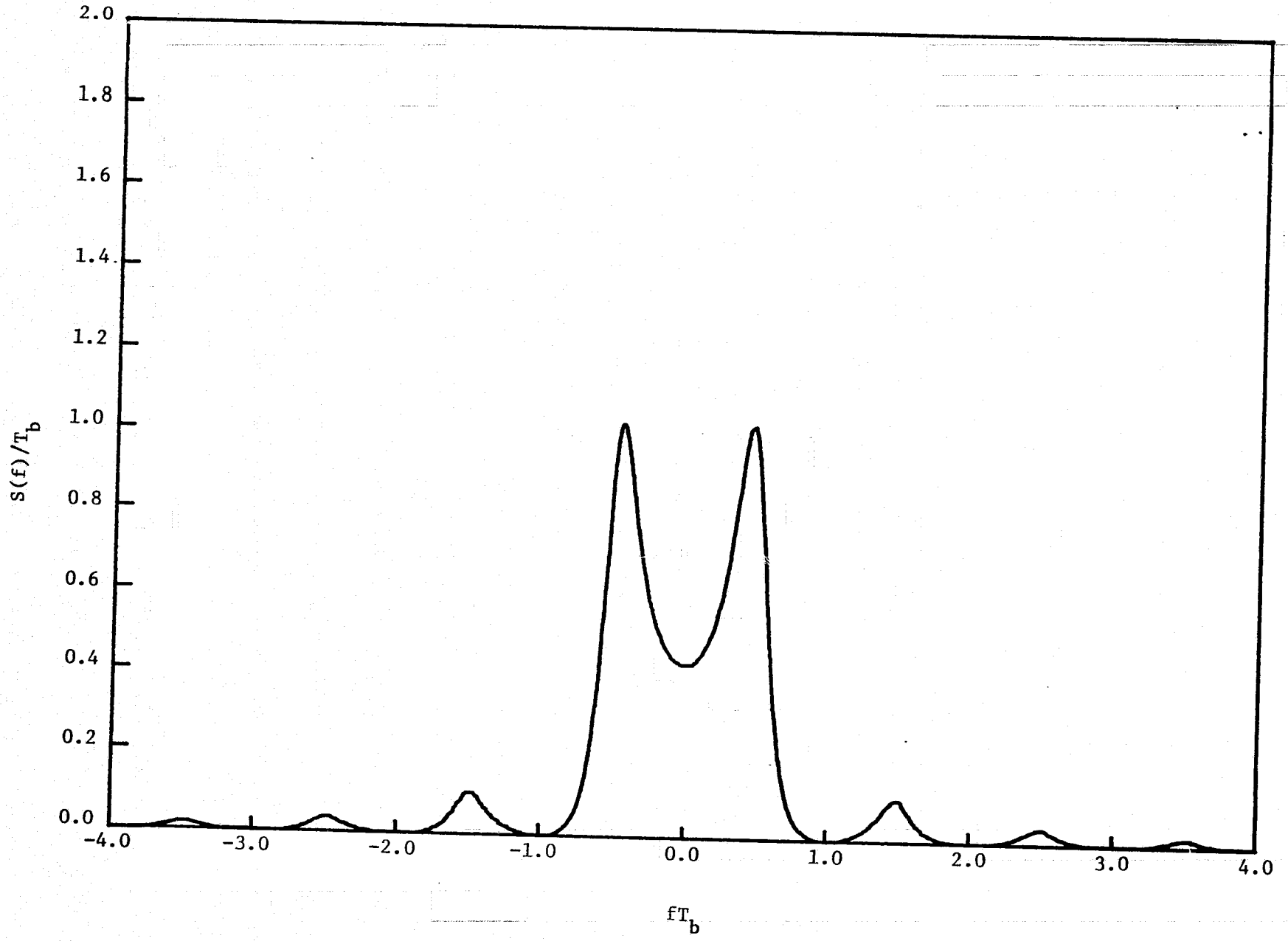

Figure 9d. Power Spectrum of First Order Markov Source; $p_t = 0.7$

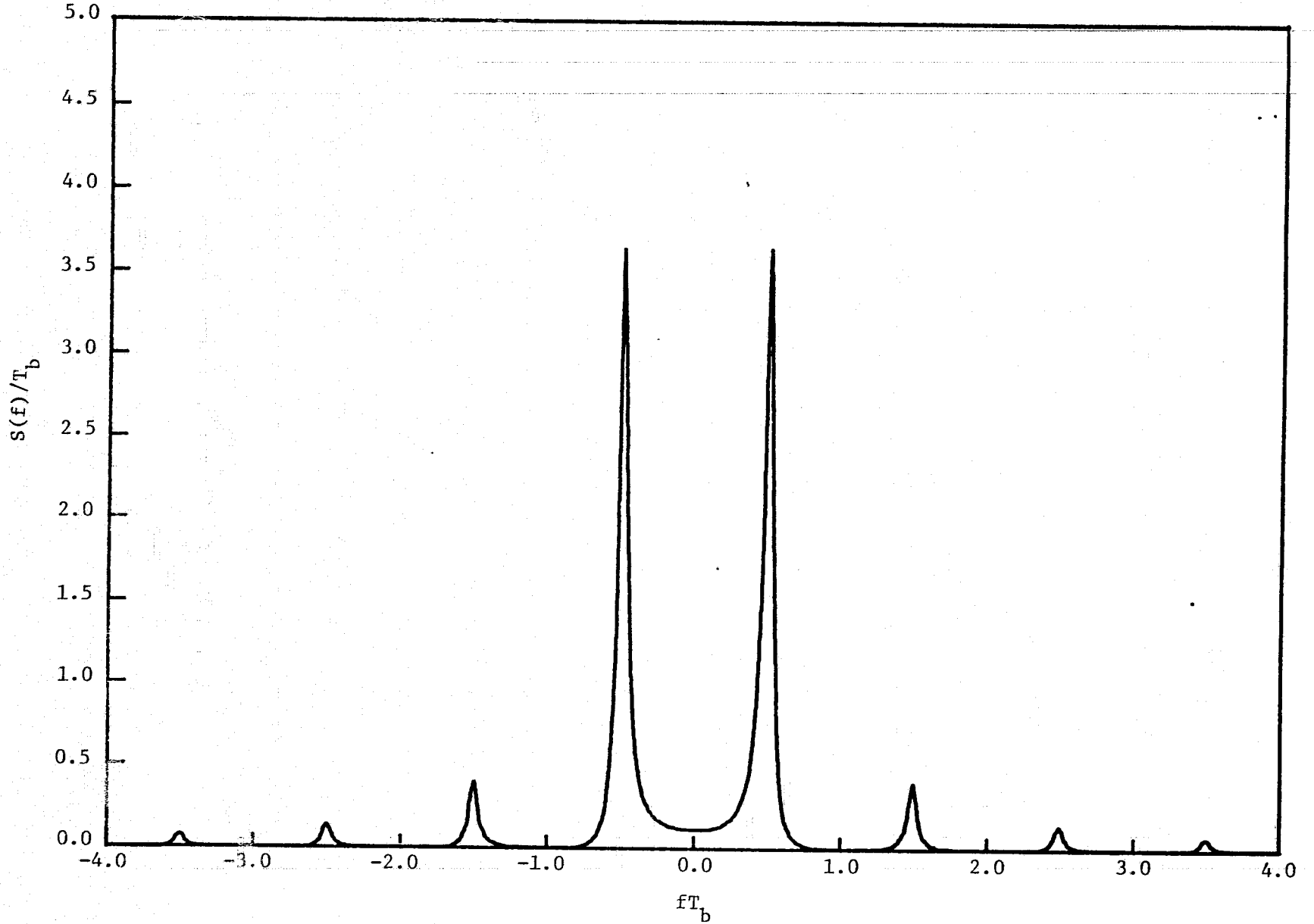

Figure 9e. Power Spectrum of First Order Markov Source; $p_t = 0.9$

As an example of the application of (62), consider the rate 1/2 constraint length 3 convolutional code described by the generator matrix of (37). The modified generator matrix $\underline{H}$ as defined by (50) is then

$$\underline{H} = \begin{bmatrix} 0 & 1 & 1 \\ 1 & 0 & 1 \end{bmatrix} \tag{66}$$

The corresponding continuous component of the encoder output spectrum may be obtained from the following closed form solution for $S_X(f)$, namely

$$S_X(f) = 1 - \frac{1}{2}\bar{t}^4 + \frac{-\bar{t}^3(1+\bar{t}-\bar{t}^2) + \bar{t}^2(1+\bar{t}^3-\bar{t}^4)\cos 4\pi fT + \bar{t}^2(1-\bar{t}-\bar{t}^2+\bar{t}^3)\cos 8\pi fT}{1 - 2\bar{t}\cos 4\pi fT + \bar{t}^2} \tag{67}$$

Fig. 10 is an illustration of $S_c(f)$ [using (67)] for several values of transition density $p_t = (1 - \bar{t})/2$. Note the unorthodox behavior of this spectrum in accordance with the similar behavior of that corresponding to the encoder input bit stream (Fig. 9).

VI. Encoder Output Spectrum in the Presence of Alternate Symbol Inversion

Alternate symbol inversion (Ref. 5) is a technique in which alternate symbols of the encoder output are inverted to provide the sufficient richness of symbol transitions necessary for adequate symbol synchronizer performance. In this section, we examine the effects of such a nonlinear operation on the power spectrum of the convolutional encoder output.

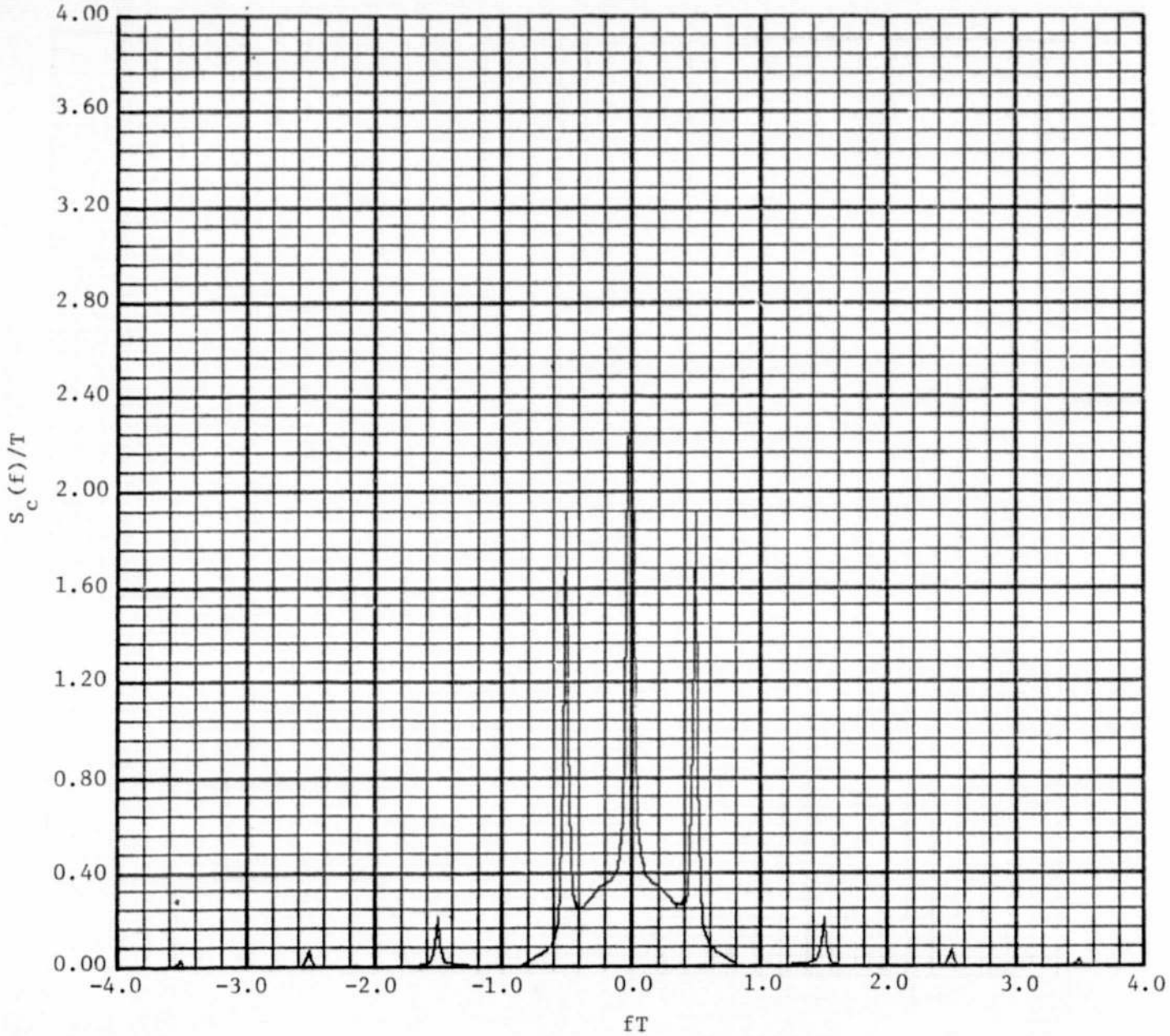

Figure 10a. Spectrum for Best Rate 1/2, Constraint Length 3 Convolutional Code; First Order Markov Source Input; $p_t = 0.1$

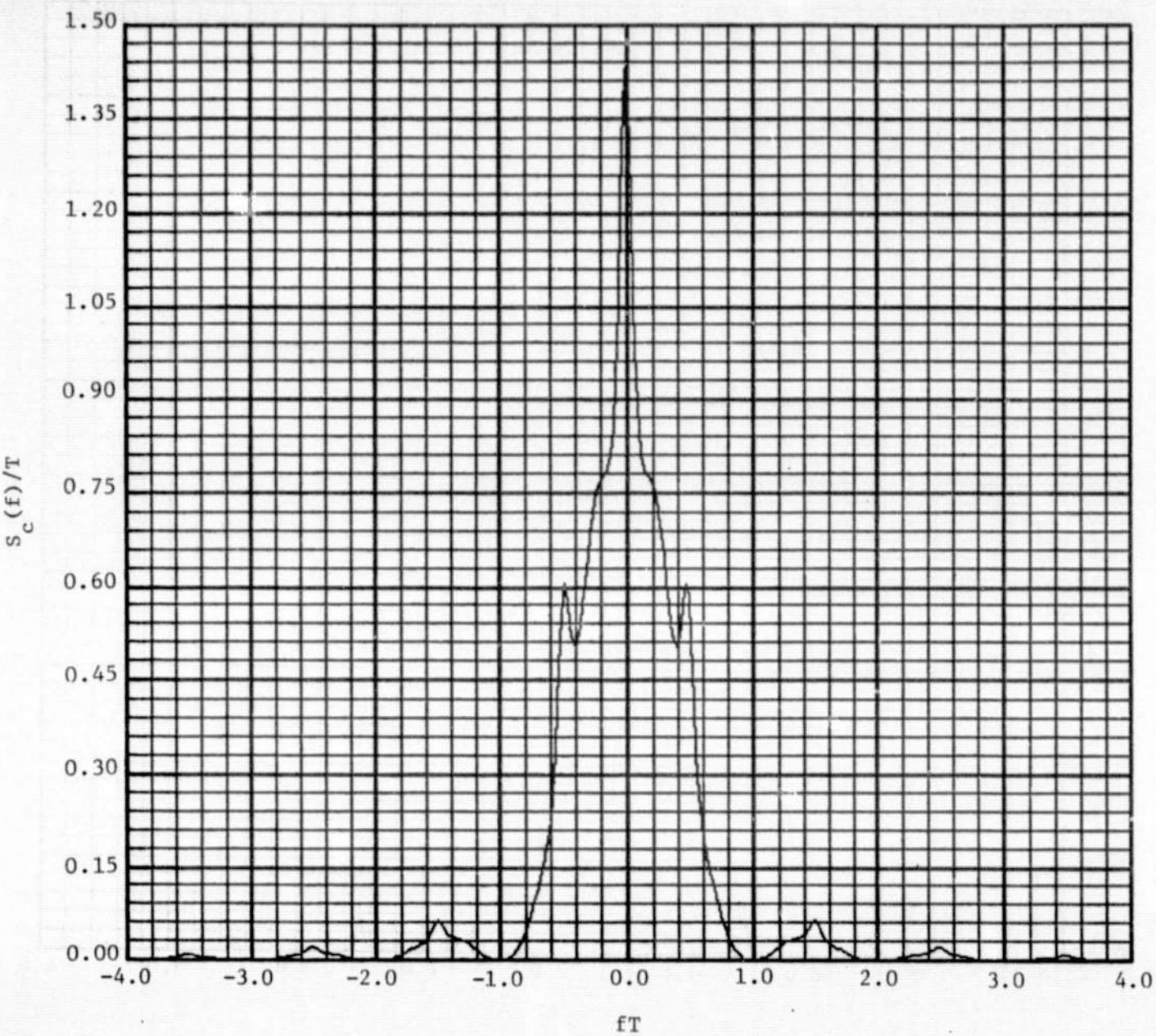

Figure 10b. Spectrum for Best Rate 1/2, Constraint Length 3 Convolutional Code; First Order Markov Source Input; $p_t = 0.3$

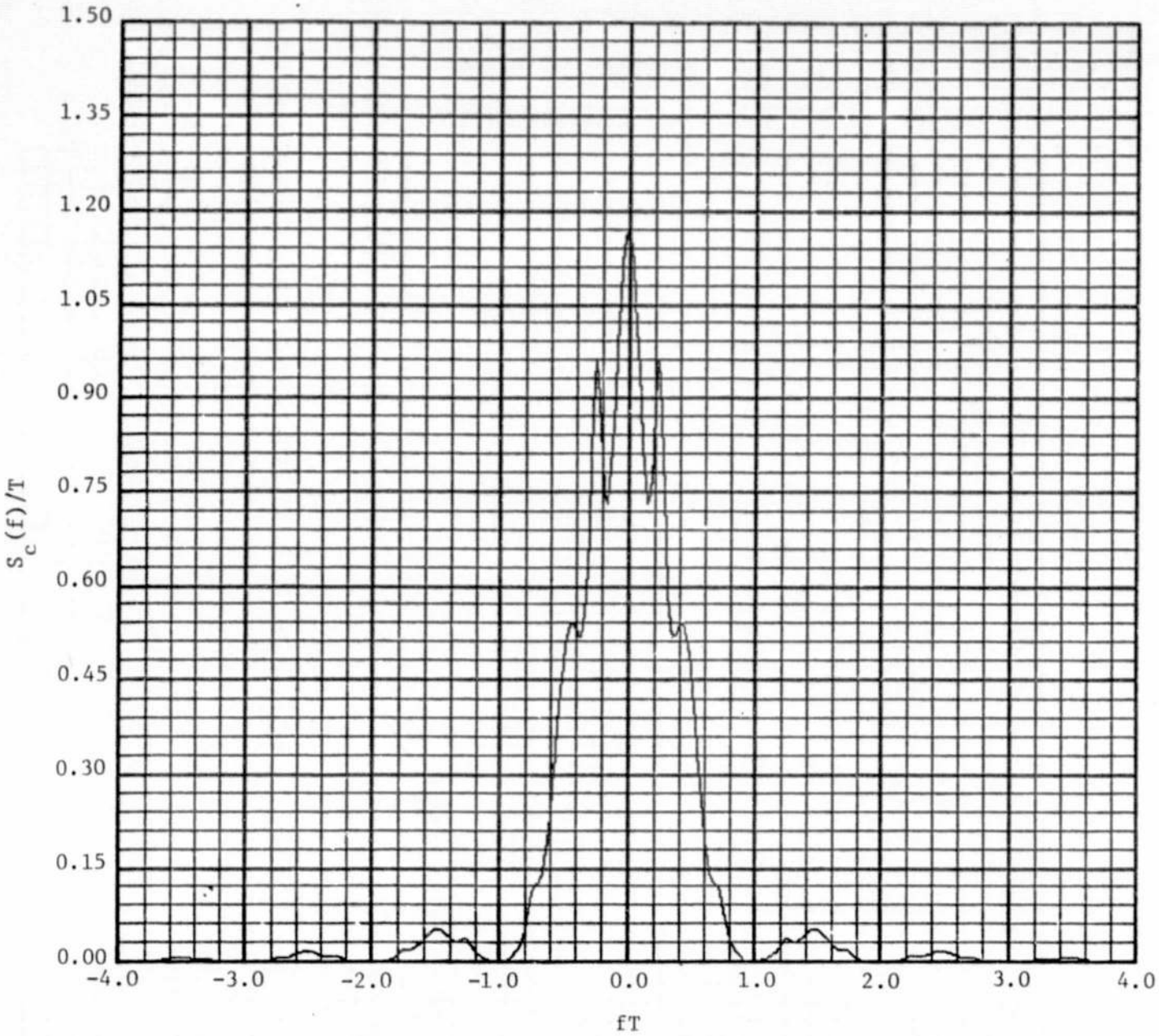

Figure 10c. Spectrum for Best Rate 1/2, Constraint Length 3 Convolutional Code; First Order Markov Source Input; $p_t = 0.7$

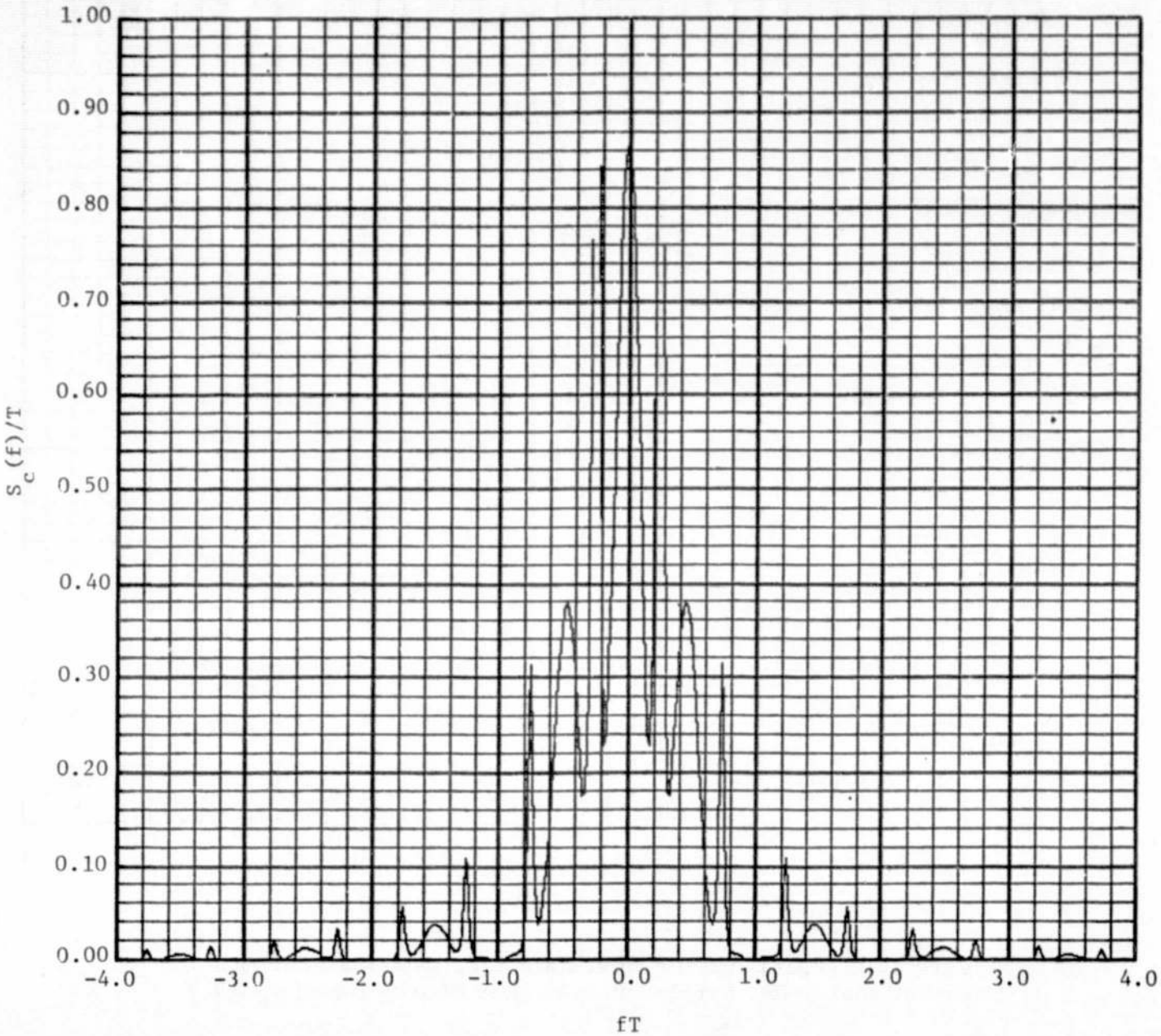

Figure 10d. Spectrum for Best Rate 1/2, Constraint Length 3 Convolutional Code; First Order Markov Source Input; $p_t = 0.9$

If the number of interleaving tap outputs is an even number, we can simply put inverters at alternate interleaving taps*, in which case the general equation (12) for $S_X(f)$ should be modified to read

$$S_X(f) = \frac{1}{n}\sum_{p=1}^{n}\sum_{q=1}^{n}(-1)^{p+q}\sum_{\ell=0}^{\infty}\epsilon_\ell \operatorname{cov}(X_p, X_{n\ell+q})\cos\left[2\pi(n\ell + q - p)fT\right] \tag{68}$$

Similarly, for computation of the discrete component of the encoder output spectrum, $S_d(f)$ of (15) remains valid with, however, $\overline{X}_p$ of (18) and (54), respectively, modified as follows:

$$\overline{X}_p = (-1)^p \bar{a}^{\alpha_p} \tag{69}$$

and

$$\overline{X}_p = (-1)^p \left(1 - h_{p,1}\right) \bar{t}^{\rho_p} \tag{70}$$

If the number of interleaving tap outputs is an odd number, we cannot put fixed inverters on alternating tap outputs. Instead, we can look at the alternate symbol inverted output as having been obtained by adding (modulo 2) an external alternating binary sequence of ones and zeros to the encoder (0, 1) output sequence. An equivalent procedure, which is more convenient for computation of the power spectrum is described as follows. Given a constraint length K, rate b/n convolutional code with n odd and generator matrix coefficients $\{g_{p,i}\}$; $p = 1, 2, \ldots, n$, $i = 1, 2, \ldots,$ Kb, we can, without any loss in

*Without any loss of generality, we assume that the first symbol inverter appears on the first tap output.

optimality or any change in transmission rate, construct an equivalent code with constraint length K and rate 2b/2n whose 2n x 2Kb generator matrix has coefficients $\{g^*_{p,j}\}$ given by

$$g^*_{p,j} = \begin{cases} g_{p-b,j}\,; & p = b+1,\ b+2,\ \ldots,\ (K+1)b \\ & j = 1,\ 2,\ \ldots,\ n \\ g_{p,j-n}\,; & p = 1,\ 2,\ \ldots,\ Kb \\ & j = n+1,\ n+2,\ \ldots,\ 2n \\ 0\,; & \text{elsewhere} \end{cases} \tag{71}$$

Fig. 11 is an illustration of this procedure for b = 1, K = 3. Now, since the number of output taps (2n) is even, we can once again use fixed alternating symbol inverters on these taps and the general results of (68), (69), and (70) apply with n replaced by 2n, b replaced by 2b, $g_{p,i}$ replaced by $g^*_{p,i}$, and using (50) $h_{p,i}$ replaced by $h^*_{p,i}$.

Before presenting a specific example, we can once again make some general statements for the various input source models previously considered. When the input is a purely random sequence, then as before the only terms which contribute to the summations in (68) are those for which p = q and $\ell = 0$. Since for these terms $(-1)^{p+q} = 1$, then (68) reduces to (12) which for this special case gives the result in (28). Thus, <u>for the class of uncorrelated convolutional codes, alternate symbol inversion has no effect on the encoder output spectrum</u>. This is intuitively pleasing since one would expect that adding an alternating sequence to a purely random sequence (the encoder output before alternate symbol inversion) should produce again a random sequence.

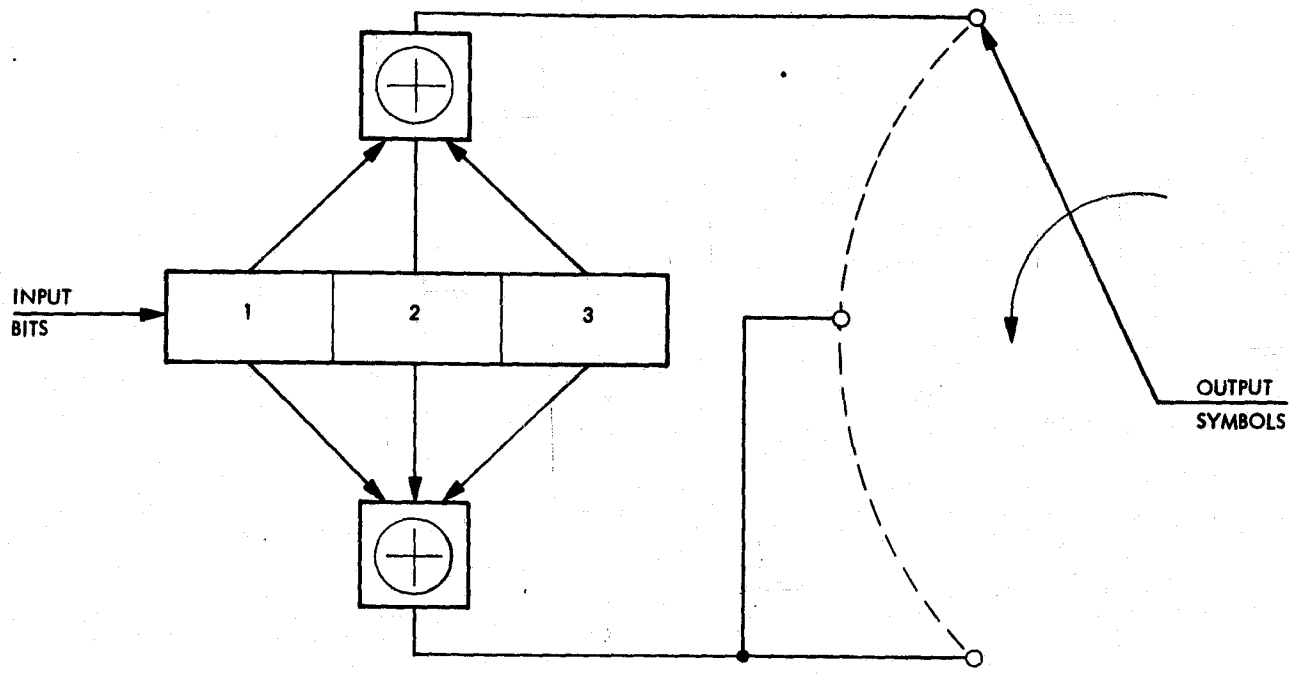

Figure 11a. An Optimum Convolutional Encoder with b = 1, n = 3, and K = 3

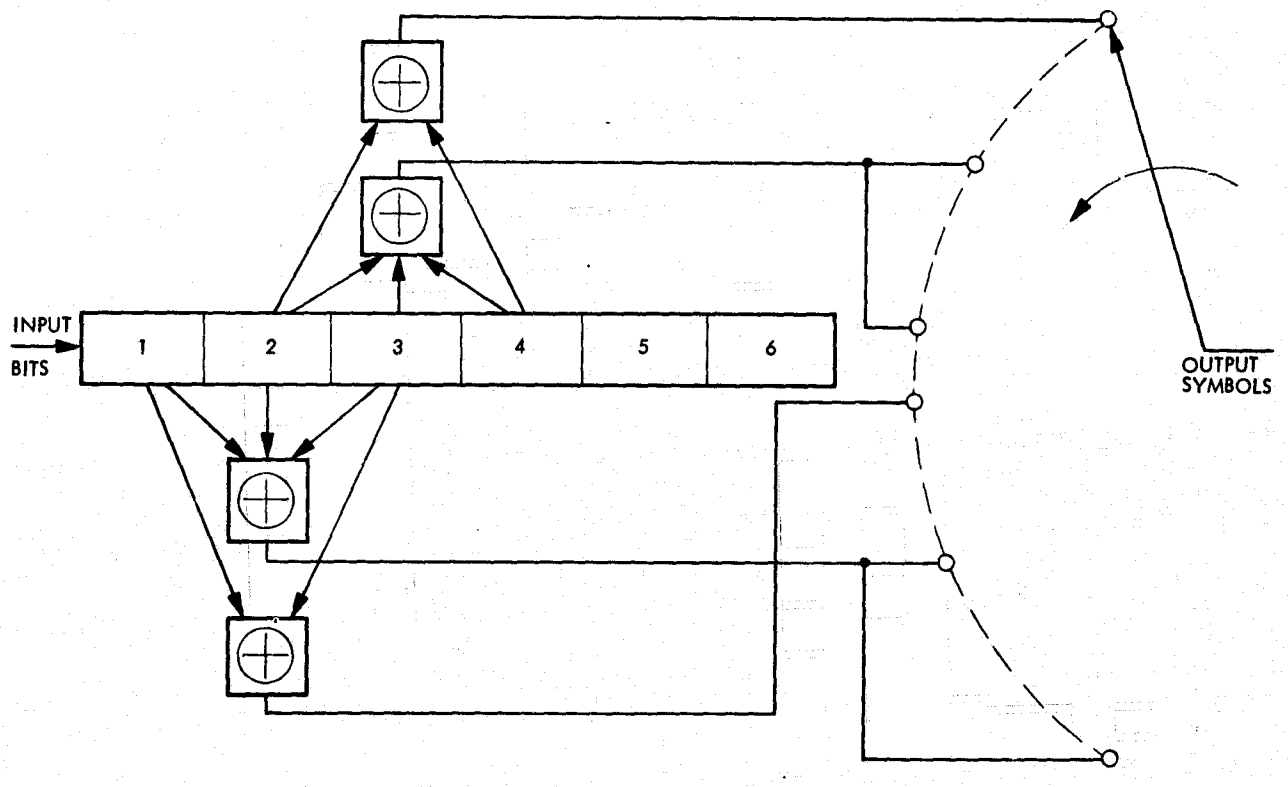

Figure 11b. An Equivalent Encoder with b = 2, n = 6, and K = 3

For correlated convolutional codes alternate symbol inversion will, in general, have a spreading effect on the output spectrum. If, however, we again consider the subclass whose generator matrix has at least two identical rows, and if the identical rows are spaced such that p+q is always <u>even</u>, then alternate symbol inversion will not affect the encoder output spectrum.

To demonstrate the spectrum spreading effect of alternate symbol inversion, consider the rate 1/4 code described by the generator matrix in (33). When alternate symbol inversion is employed and the input is a random NRZ sequence, (34) is modified to

$$S_X(f) = 1 + \frac{1}{2}\left[-2\cos 2\pi fT + \cos 4\pi fT\right] \tag{72}$$

and the corresponding output spectrum is illustrated in Figure 12. This figure should be compared to Figure 4 which characterizes the same encoder output without alternate symbol inversion.

Another illustration of the effect appears in Figures 13a and 13b where the optimum K = 7 rate 1/2 code is employed with an unbalanced NRZ input having $p^* = 0.2$. Figure 13a is essentially a duplication of Figure 7b with, however, the discrete component of the output spectrum superimposed. Similarly, Figure 13b has the discrete spectrum superimposed. Notice how alternate symbol inversion not only spreads the spectrum but also creates many new significant discrete spectral harmonics.

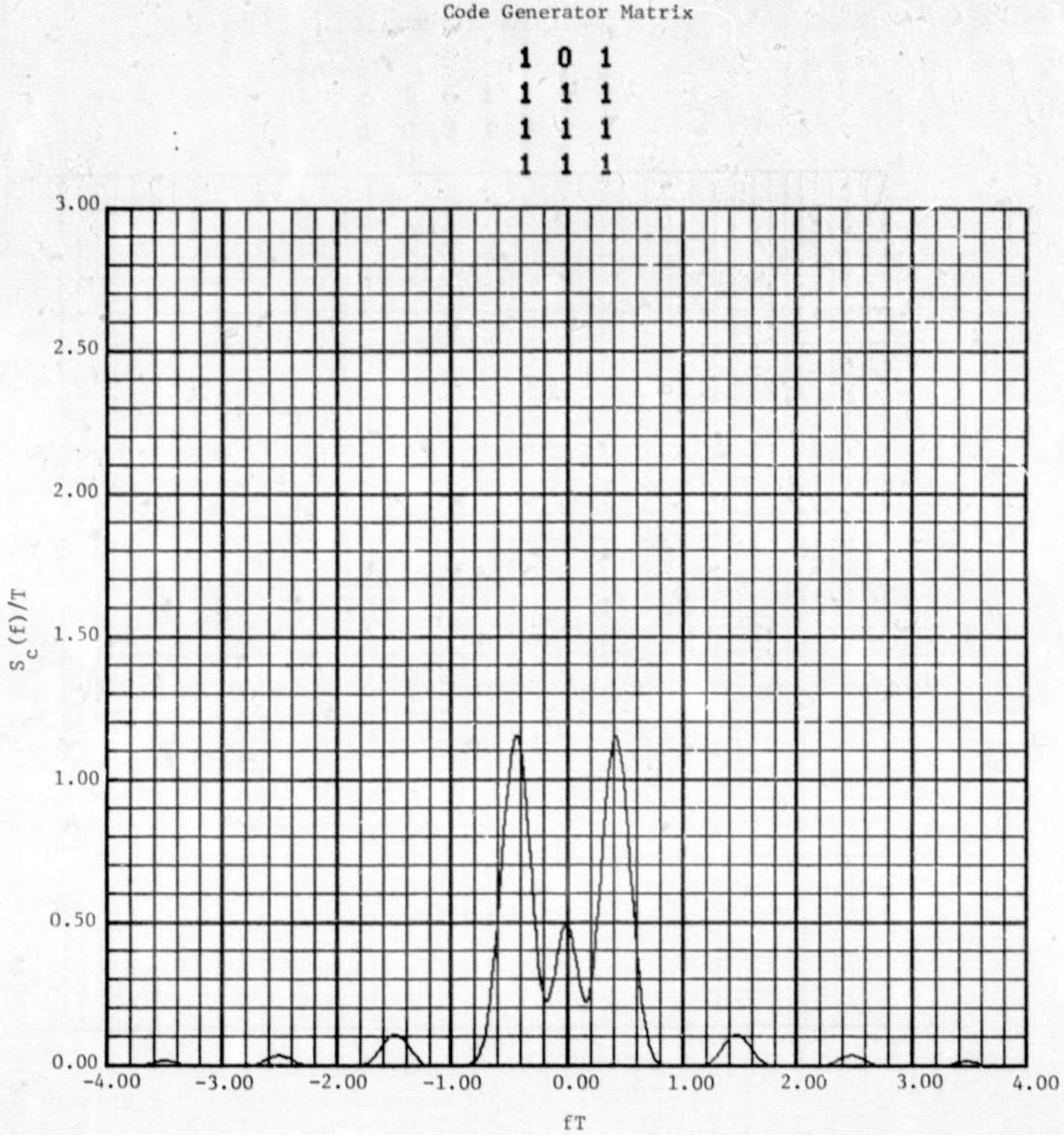

Figure 12. Spectrum for Best Rate 1/4, Constraint Length 3 Convolutional Code; (Alternate Symbol Inversion)

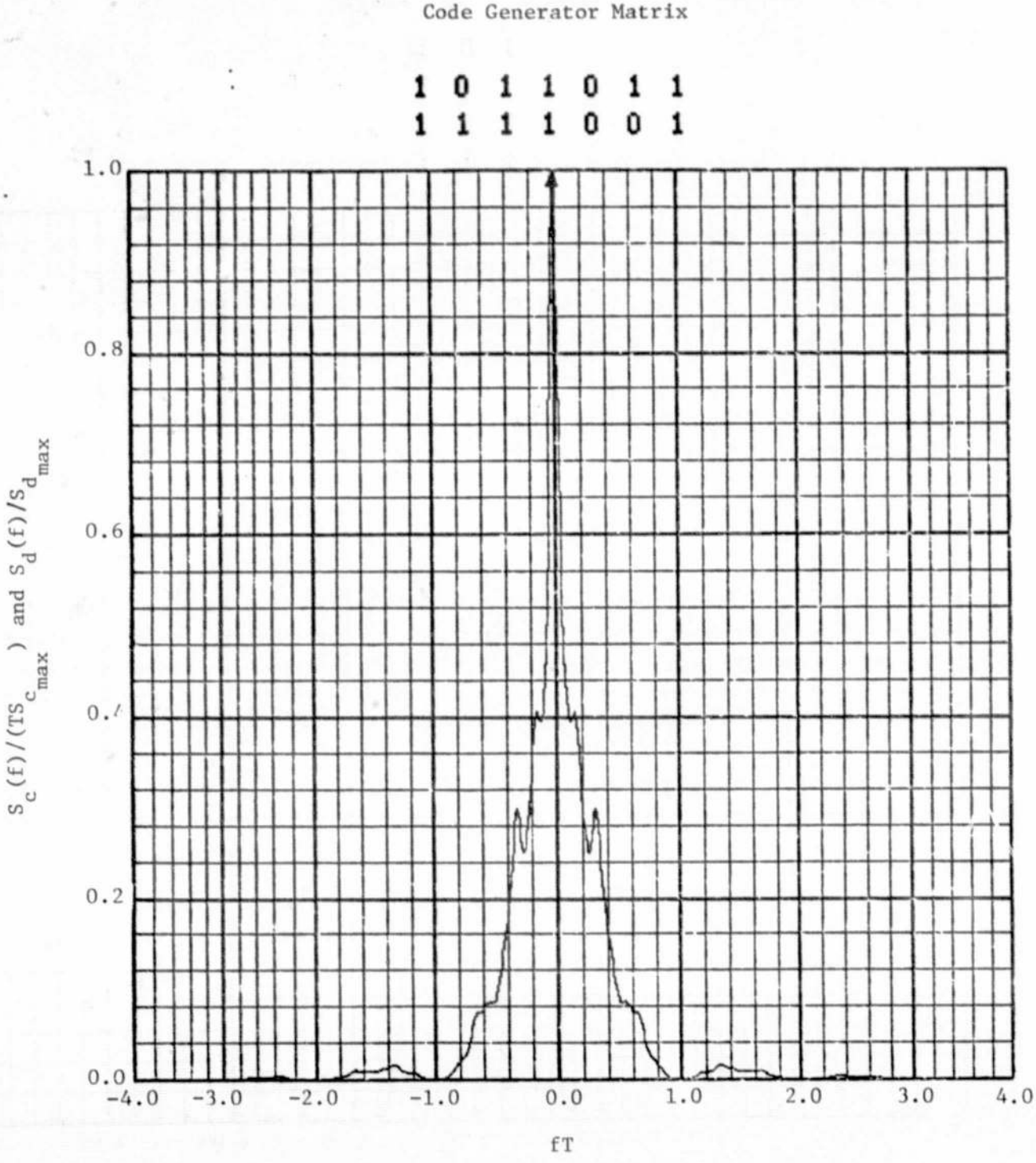

Figure 13a. Output Spectrum of the Code With Unbalanced NRZ Input;
$p^* = 0.2$; $S_{c_{max}} = 2.398$; $S_{d_{max}} = 0.006$

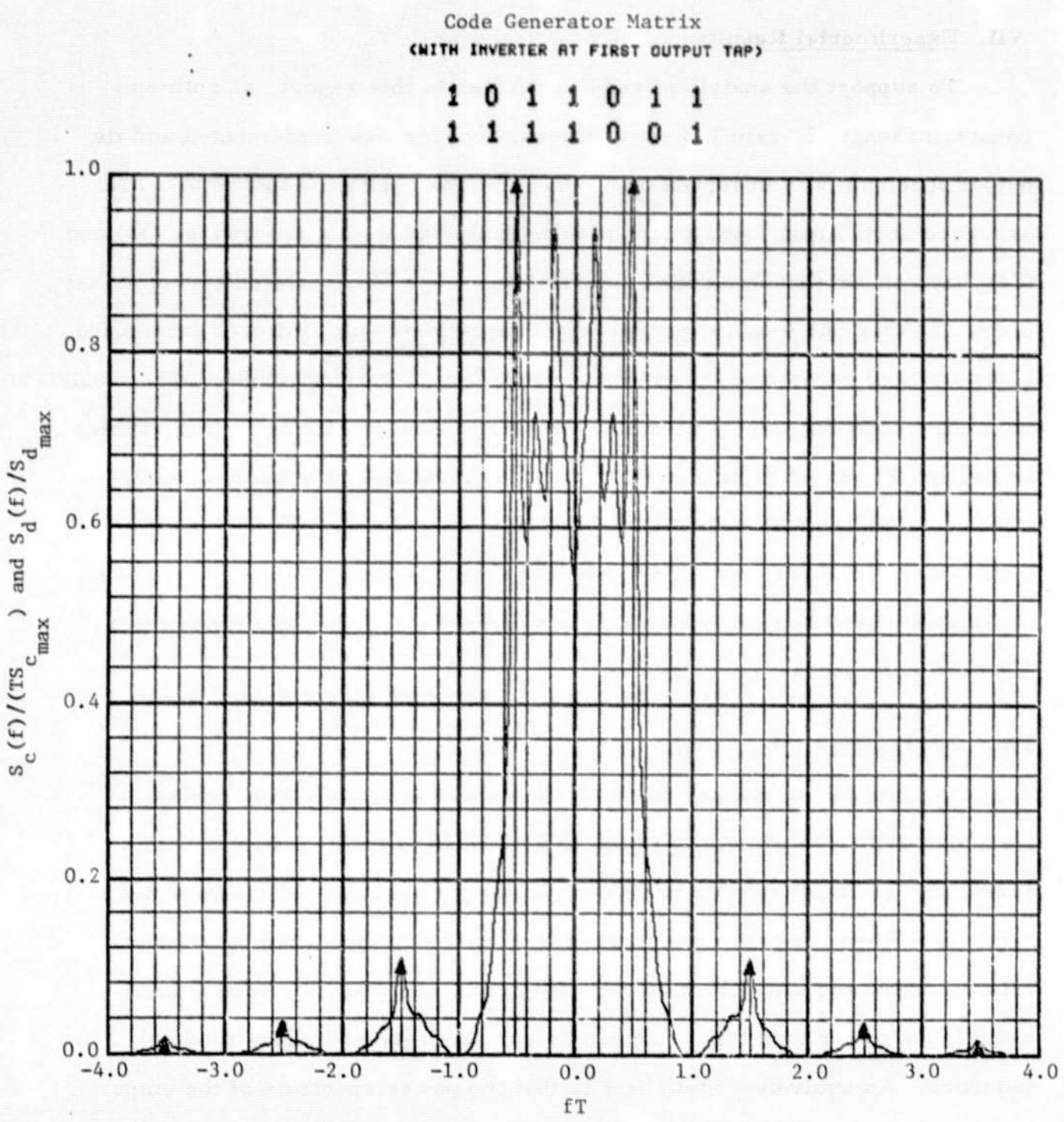

Figure 13b. Output Spectrum of the Code with Unbalanced NRZ Input; (Alternate Symbol Inversion)
$p^* = 0.2$; $S_{c_{max}} = 0.985$; $S_{d_{max}} = 0.002$

VII. Experimental Results

To support the analytical results derived in this report, an optimum constraint length 3, rate 1/4 convolutional encoder was implemented, and its output spectrum was observed on a spectrum analyzer in response to a PN sequence at its input. Analytical results contained in this report [see (33) and (34)] have shown that this code belongs to the class of correlated convolutional codes and thus one would expect an output spectrum which differed from a frequency scaled version of the input spectrum [see Figure 4]. Indeed this result is confirmed by the experimental results illustrated in Figure 14 (logarithmic scale) and Figure 15 (linear scale). Unlike a rate 1/4 uncorrelated convolutional code whose 3 dB bandwidth of the output spectrum is four times the 3 dB bandwidth of its input, the 3 dB bandwidth of the output spectrum of this best constraint length 3, rate 1/4 code is less than one and one-half times the 3 dB bandwidth of its input.

VIII. Observations and Conclusions

We have observed that there exists a class of convolutional codes (designated correlated convolutional codes) which have the property that a purely random input results in an encoder output sequence with correlated symbols. When the power spectrum of the waveform produced by this correlated output sequence is computed, it is observed that its effective bandwidth is narrower than that produced by an uncorrelated (purely random) sequence. An equivalent statement is that the power spectrum of the output waveform corresponding to the entire (doubly infinite) sequence is narrower than that for the individual pulse, the latter being identical to the power spectrum of an equivalent pulse stream with uncorrelated symbols.

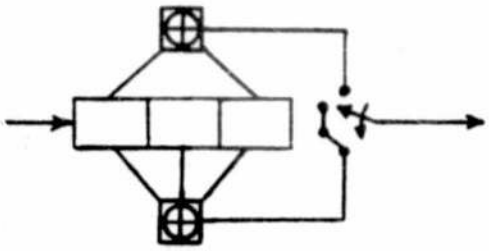

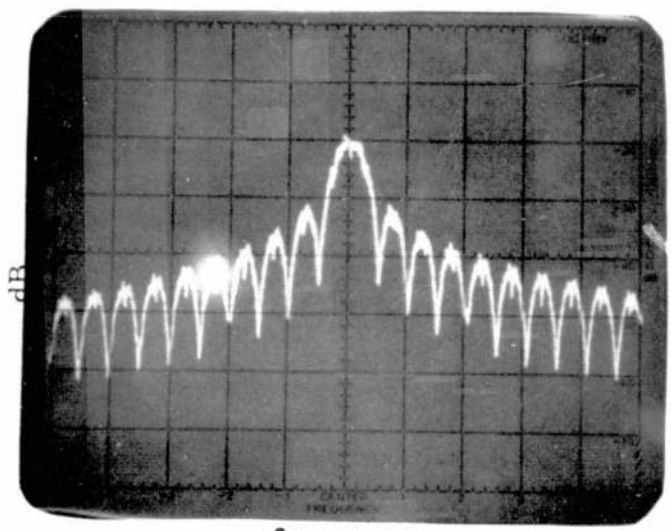

a. Input Spectrum (PN Sequence)

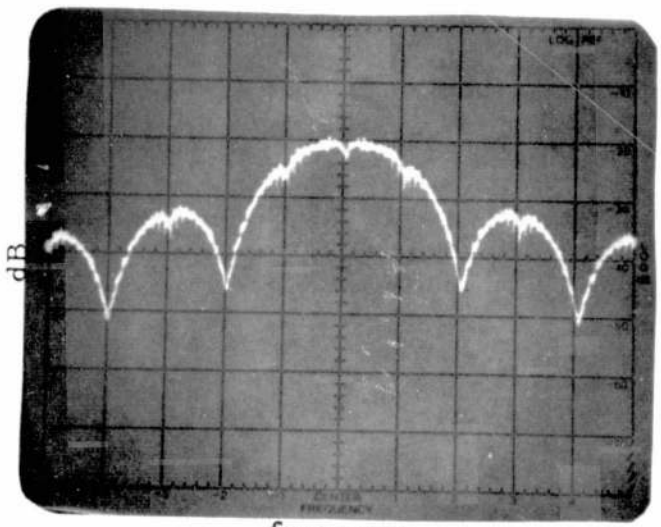

b. Output Spectrum of rate 1/4 Uncorrelated Convolutional Code

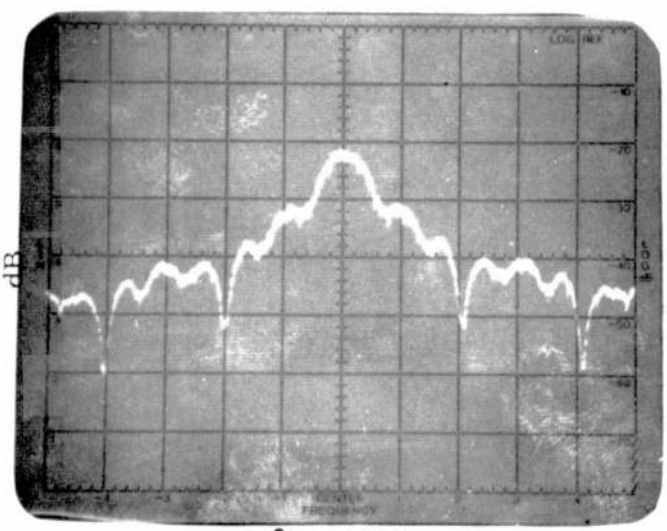

c. Code Output Spectrum

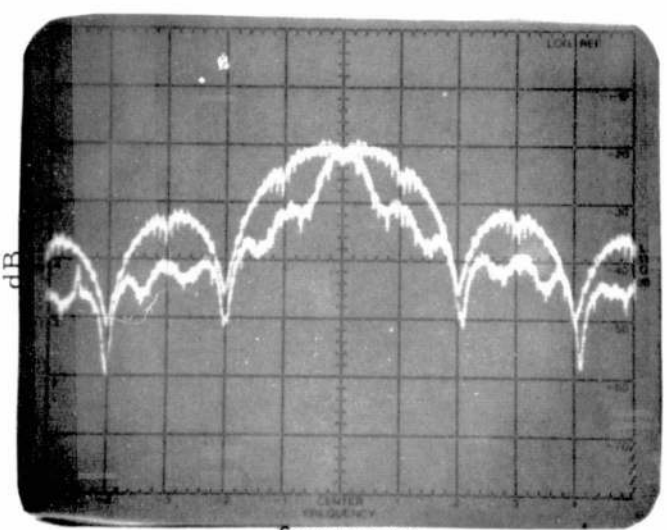

d. Comparison between Fig. 14b and Fig. 14c

Figure 14. Experimental Measurement of Input and Output Spectra for Best Rate 1/4, Constraint length 3, Convolutional Code (Logarithmic Scale)

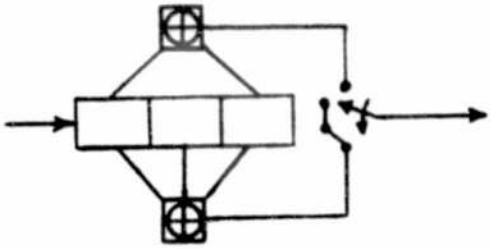

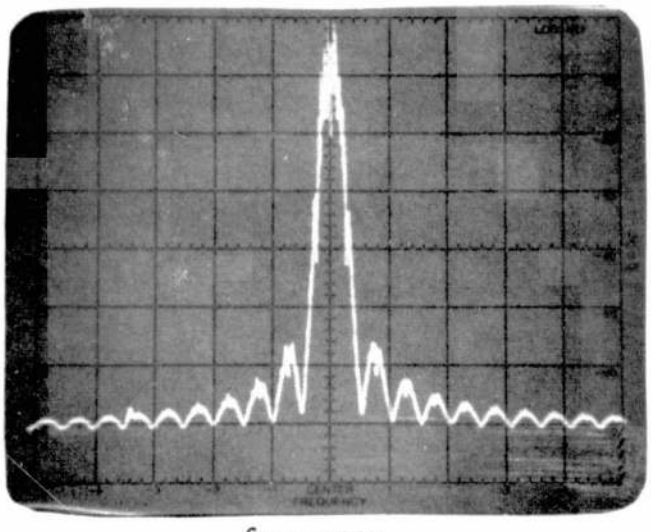

frequency

a. Input Spectrum (PN Sequence)

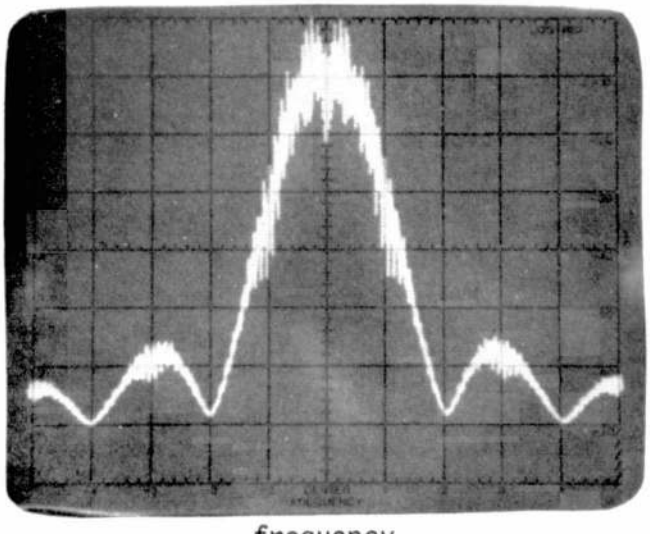

frequency

b. Output Spectrum of rate 1/4 Uncorrelated Convolutional Code

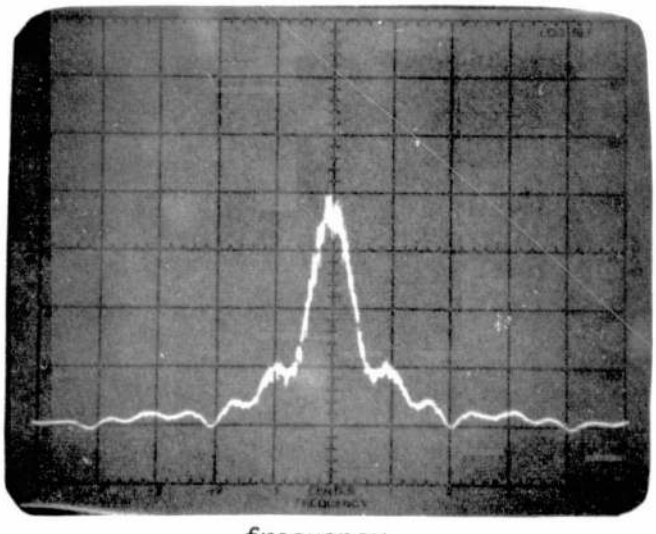

frequency

c. Code Output Spectrum

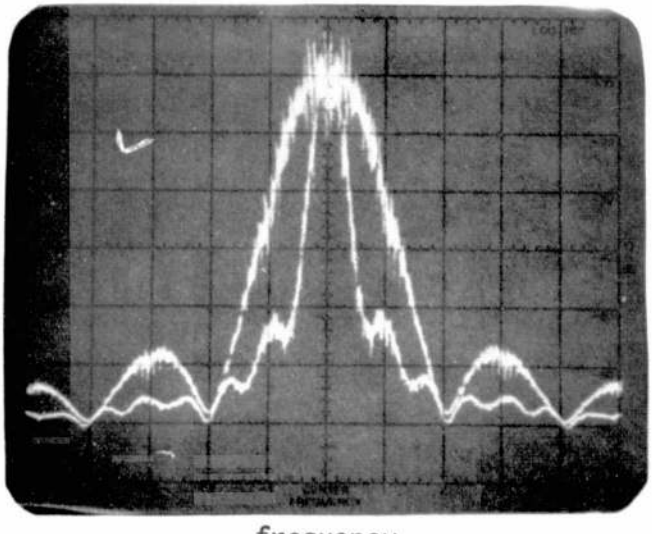

frequency

d. Comparison between Fig. 15b and Fig. 15c

Figure 15. Experimental Measurement of Input and Output Spectra for Best Rate 1/4, Constraint length 3, Convolutional Code (Linear Scale)

Based upon the above, one might hasten to conclude that to achieve a given error probability performance, it might be possible to go to a short constraint length, high rate code (less complexity) without having to pay the bandwidth expansion penalty ordinarily associated with this choice. Unfortunately, this is not the case. The reason is that the transmit filter and channel bandwidths are determined by the need to pass an individual pulse with minimum distortion; this is necessary for adequate symbol sync performance in the receiver prior to decoding. Indeed, the bandwidth of the power spectrum corresponding to an individual output symbol pulse expands directly as the reciprocal of the code rate. Thus, the correlation of the output symbols is not effective in reducing the channel bandwidth requirements. However, portions of the receiver, e.g., the carrier tracking loop, whose performance depends on the bandwidth occupancy of the entire modulation (as opposed to that of an individual pulse) can be aided by employing correlated convolutional codes. For example, if the transmission is suppressed carrier and the carrier reconstruction loop is a Costas loop, then a reduction in the bandwidth of the modulation enables one to design narrower arm filters thereby improving the loop's squaring loss (tracking threshold) performance. An example of this point is illustrated by the results of Figure 16 where a Costas loop with single pole RC arm filters has been assumed. The corresponding analysis which generated the curves in this figure is contained in Appendix B.

Before leaving this subject, we remind the reader that if alternate symbol inversion is employed to improve the encoder output symbol transition density, then this acts in such a way as to once again expand bandwidth and the above spectral advantage associated with correlated convolutional codes tends to disappear.

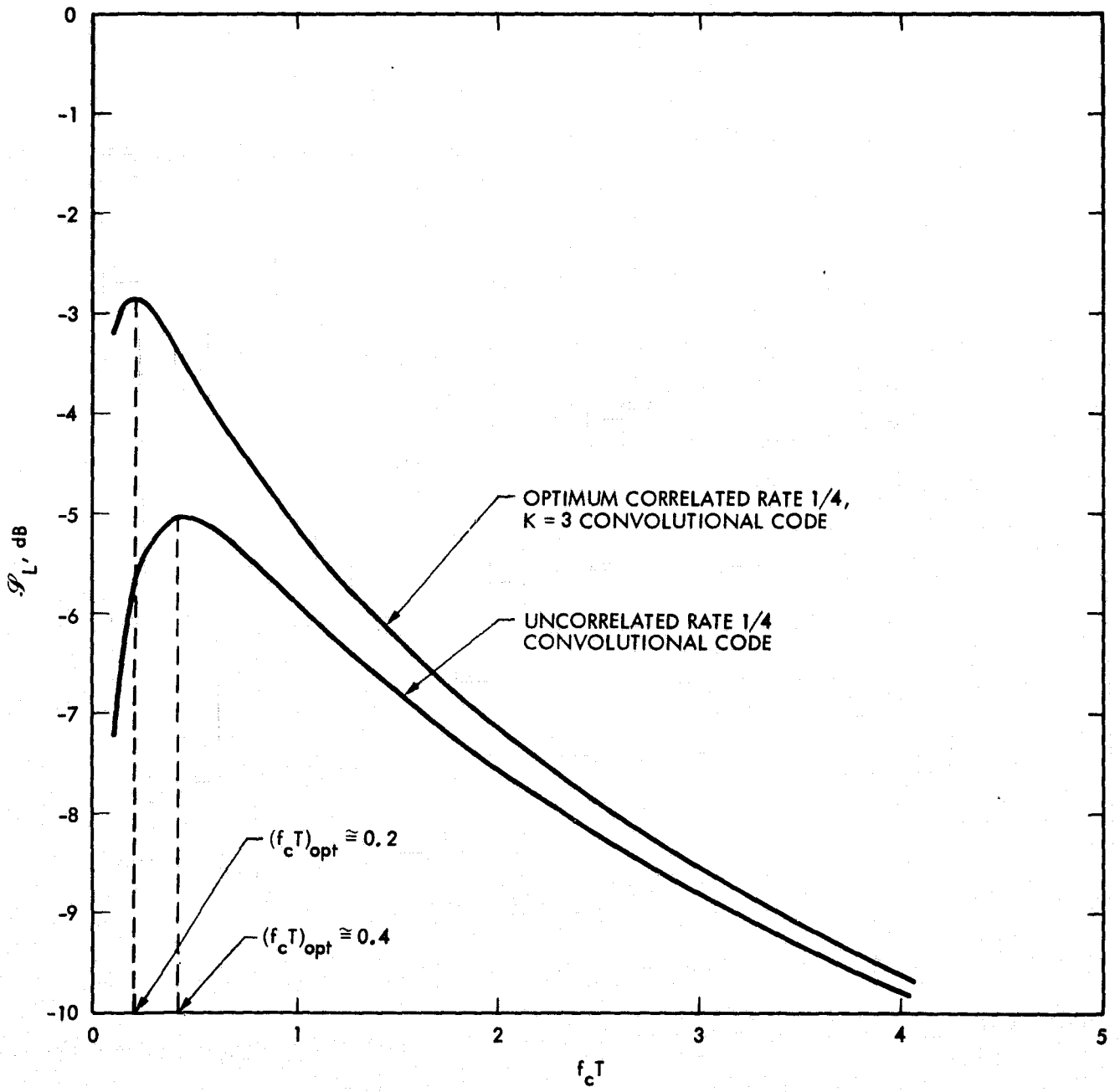

Figure 16. Squaring Loss versus the Ratio of 3 dB Cutoff Frequency to Data (Symbol) Rate: Detection Symbol Signal-to-Noise Ratio ST/N_0 = -4 dB

REFERENCES:

(1) Franks, L. E., Signal Theory, Prentice-Hall, Inc., Englewood Cliffs, N.J., 1969.

(2) Larsen, K. J., "Short Convolutional Codes with Maximal Free Distance for Rates 1/2, 1/3, and 1/4," IEEE Transactions on Information Theory, Vol. IT-19, No. 3, May, 1973, pp. 371-372.

(3) Odenwalder, J. P., "Optimal Decoding of Convolutional Codes," PhD Dissertation, University of California, Los Angeles, 1970.

(4) Lindsey, W. C., and Simon, M. K., Telecommunication Systems Engineering, Prentice-Hall, Inc., Englewood Cliffs, N.J., 1973.

(5) Deep Space Network/Flight Project Interface Design Handbook, Report 810-5; Rev. D. March 15, 1978 (JPL internal document).

(6) Jolley, L. B. W., Summation of Series, Dover Publications, New York, N.Y., 1961.

(7) Levitt, B. K., "Power Spectrum for Binary NRZ Data with less than 50 percent Transitions," JPL DSN Progress Report 42-32, April 15, 1976, pp. 86-89.

(8) Simon, M. K., and Lindsey, W. C., "Optimum Performance of Suppressed Carrier Receivers with Costas Loop Tracking," IEEE Transactions on Communications, Vol. COM-25, No. 2, February, 1977, pp. 215-227.

APPENDIX A

THE COMPUTATION OF POWER SPECTRAL DENSITY FOR SYNCHRONOUS DATA PULSE STREAMS

Introduction

Many techniques appear in the literature and some textbooks for the computation of the power spectral density of a synchronous data pulse stream where the underlying data sequence which generates the pulse stream has known statistical properties. In all cases found by the author thus far, the sequence is assumed to be either wide sense stationary (WSS) with known auto-correlation function or more generally an N-ary Markov source with known (fixed) stationary and transition probabilities. A special case of the latter is a purely random source, i.e., one that emits an elementary signal (pulse) in a given signaling interval independent of those emitted in previous signaling intervals. Such a source can be modeled as a degenerate case of an N-ary Markov source whose NXN transition matrix (the matrix of transition probabilities) has identical rows. When N = 2, and the two elementary signals are the same, we get the familiar results for antipodal binary signaling.

Occasionally, one finds situations where the generating data sequence is not WSS but, however, is cyclostationary, i.e., its first two moments are periodic. One such case occurs at the output of a convolutional encoder where the period (in code symbols) is equal to the reciprocal of the code rate. Thus, in order to characterize the spectral properties of the output of such an encoder, one must develop an expression for the power spectral density of a synchronous data stream whose generating sequence is cyclostationary. Such is the primary purpose of this appendix. As a review and an introduction to the technique, we

shall first present the derivation of the known result for the power spectral density of a synchronous data stream generated by a binary WSS sequence.

Power Spectral Density of a Synchronous Data Stream Generated by a Binary, Zero Mean, WSS Sequence

Consider the binary (±1) zero mean, WSS sequence a_n for which it is known that

$$\overline{a_n} = 0$$

$$\overline{a_n a_m} = R(m - n) \tag{A-1}$$

and the overbar denotes statistical expectation. From this sequence, we form the synchronous data pulse stream

$$m(t) = \sum_{n=-\infty}^{\infty} a_n \, p(t - nT) \tag{A-2}$$

where p (t) is the elementary signal (pulse shape) and is not necessarily restricted to be time-limited to only a single signaling interval, i.e., the pulse train m (t) can contain overlapping pulses. Irrespective of the properties of the generating sequence $\{a_n\}$, the data stream m (t) is itself cyclostationary since the expected value of the product m (t) m $(t + \tau)$ is, in addition to being a function of τ, a periodic function of t. Thus, to compute the power spectral density $S_m(f)$ of m (t), we must first average

$$R(t;\tau) \triangleq \overline{m(t)\, m(t + \tau)} \tag{A-3}$$

over t [the averaging is performed over the period of R (t ; τ)] and then take the Fourier transform of the result. Thus,

$$S_m(f) \triangleq \mathcal{F}\{\langle R\ (t\ ;\ \tau)\rangle\} \tag{A-4}$$

where $\langle\ \rangle$ denotes time average and $\mathcal{F}$ denotes Fourier transform. Substituting (A-2) into (A-3) and making use of (A-1) and the definition of Fourier transform, we get*

$$S_m(f) = \int_\tau \left\langle \sum_n \sum_m R\ (m - n)\ p\ (t - nT)\ p\ (t + \tau - mT) \right\rangle e^{-j2\pi f\tau} d\tau \tag{A-5}$$

Since

$$p\ (t) = \int_{-\infty}^{\infty} P(f)\ e^{j2\pi ft}\ df \tag{A-6}$$

where P (f) is the Fourier transform of p (t), then substituting (A-6) in (A-5) gives

$$S_m(f) = \int_y \int_z \sum_n \sum_m R\ (m - n)\ P(y)\ P^*\ (z) e^{-j2\pi ynT}$$

$$\times\ e^{j2\pi zmT} \left\langle e^{j2\pi(y-z)t} \right\rangle \int_\tau e^{-j2\pi(f+z)\tau} d\tau\ dy\ dz \tag{A-7}$$

*Unless otherwise noted, all summations and integrals range from $-\infty$ to ∞.

where the asterisk denotes complex conjugate. Recalling that

$$\int_{\tau} e^{-j2\pi x\tau}\, d\tau = \delta(x) \tag{A-8}$$

then (A-7) simplifies to

$$S_m(f) = \int_y \sum_n \sum_m R(m-n)\, P(y)\, P^*(-f)\, e^{-j2\pi ynT}\, e^{-j2\pi fmT} \left\langle e^{j2\pi(y+f)t} \right\rangle dy$$

$$= \int_y \sum_n \sum_m R(m-n)\, P(y)\, P^*(-f)\, e^{-j2\pi f(m-n)T}\, e^{-j2\pi(y+f)nT}$$

$$\times \left\langle e^{j2\pi(y+f)t} \right\rangle dy \tag{A-9}$$

Since $R(t;\tau)$ is periodic in t with period T, then

$$\left\langle e^{j2\pi(y+f)t} \right\rangle \triangleq \frac{1}{T} \int_{\frac{-T}{2}}^{\frac{T}{2}} e^{j2\pi(y+f)t}\, dt = \frac{\sin\left[\pi(y+f)T\right]}{\pi(y+f)T} \tag{A-10}$$

Substituting (A-10) in (A-9) and letting $\ell = m - n$, gives

$$S_m(f) = \sum_{\ell} R(\ell)\, e^{-j2\pi f\ell T} \int_y P(y)\, P^*(-f)\, \frac{\sin \pi(y+f)T}{\pi(y+f)T}$$

$$\times \sum_n e^{-j2\pi(y+f)nT}\, dy \tag{A-11}$$

Finally, from Poisson's sum formula, we have that

$$\sum_{n} e^{-j2\pi xnT} = \frac{1}{T} \sum_{k} \delta\left(x - \frac{k}{T}\right) \tag{A-12}$$

which when substituted in (A-11) yields

$$S_m(f) = \left[\sum_{\ell} R(\ell)\, e^{-j2\pi f \ell T} \right] \frac{1}{T} \sum_{k} P\left(-f + \frac{k}{T}\right) P^*(-f) \frac{\sin \pi k}{\pi k} \tag{A-13}$$

Since

$$\frac{\sin \pi k}{\pi k} = \begin{cases} 1\,; & k = 0 \\ 0\,; & \text{otherwise} \end{cases} \tag{A-14}$$

and $|P(f)|^2$ is an even function of f, we get the desired result

$$\boxed{S_m(f) = S_p(f)\, S_a(f)} \tag{A-15}$$

where

$$\boxed{S_p(f) \triangleq \frac{1}{T} |P(f)|^2} \tag{A-16}$$

is the power spectral density of the individual pulse p (t) and

$$\boxed{S_a(f) \triangleq \sum_{\ell=-\infty}^{\infty} R(\ell)\, e^{-j2\pi f \ell T}} \tag{A-17}$$

is the spectral density of the sequence, i.e., the discrete Fourier transform of its correlation function. Note that if the data sequence is purely random, i.e.,

$$\overline{a_n a_m} = \begin{cases} 1 ; & m = n \\ 0 ; & \text{otherwise} \end{cases} \tag{A-18}$$

then equivalently from (A-1)

$$R(\ell) = \begin{cases} 1 ; & = 0 \\ 0 ; & \text{otherwise} \end{cases} \tag{A-19}$$

and from (A-17),

$$S_a(f) = 1 \tag{A-20}$$

Hence,

$$S(f) = S_p(f) \tag{A-21}$$

which is a commonly used result.

Power Spectral Density of a Synchronous Data Stream Generated by a Binary, Zero Mean, Cyclostationary Sequence

Suppose now that we have a binary sequence $\{a_n\}$ which has the properties

$$\overline{a_n} = 0$$

$$\overline{a_n a_m} = R(n ; m - n) \tag{A-22}$$

Furthermore,

$$R(n\,;\,m-n) = R(n+kN\,;\,m-n)\,; \qquad k = 0, \pm 1, \pm 2, \ldots \tag{A-23}$$

where N denotes the period of the correlation function R (n ; m - n). Then, following the steps leading up to (A-9), we see that the analogous result is now

$$S_m(f) = \int_y \sum_n \sum_m R(n\,;\,m-n)\; P(y)\, P^*(-f)\, e^{-j2\pi f(m-n)T}\, e^{-j2\pi(y+f)nT} \times \left\langle e^{j2\pi(y+f)t} \right\rangle dy \tag{A-24}$$

Thus far, we have not made use of the cyclostationary property given in (A-23). If now we use this property to evaluate the sum on n in (A-24), and as before let $\ell = m - n$, then it can be easily shown that

$$\sum_n R(n\,;\,\ell)\, e^{-j2\pi(y+f)nT} = \left[\sum_{n=1}^{N} R(n\,;\,\ell)\, e^{-j2\pi(y+f)nT} \right] \times \sum_k e^{-j2\pi(y+f)kNT} \tag{A-25}$$

or making use of (A-12),

$$\sum_n R(n\,;\,\ell)\, e^{-j2\pi(y+f)nT} = \left[\sum_{n=1}^{N} R(n\,;\,\ell)\, e^{-j2\pi(y+f)nT} \right] \times \frac{1}{NT} \sum_k \delta\left(y + f - \frac{k}{NT}\right) \tag{A-26}$$

Substituting (A-26) in (A-24) and performing the integration on y gives

$$S_m(f) = \frac{1}{NT} \sum_k \sum_\ell \left[\sum_{n=1}^{N} R(n;\ell)\, e^{-j2\pi nk/N} \right] e^{-j2\pi f \ell T}$$

$$\times P(-f + \frac{k}{NT})\, P^*(-f) \left\langle e^{j2\pi kt/NT} \right\rangle \qquad \text{(A-27)}$$

Since $R(t;\tau)$ is now periodic in t with period $\underline{NT}$, then

$$\left\langle e^{j2\pi kt/NT} \right\rangle \triangleq \frac{1}{NT} \int_{\frac{-NT}{2}}^{\frac{NT}{2}} e^{j2\pi kt/NT}\, dt = \frac{\sin \pi k}{\pi k} = \begin{cases} 1\,; & k = 0 \\ 0\,; & k \neq 0 \end{cases} \qquad \text{(A-28)}$$

Finally, substituting (A-28) into (A-27) gives the desired result

$$\boxed{S_m(f) = S_p(f)\, S_{\underline{a}}(f)} \qquad \text{(A-29)}$$

where $S_p(f)$ is still given by (A-16) and $S_{\underline{a}}(f)$ is defined by

$$\boxed{S_{\underline{a}}(f) = \sum_{\ell=-\infty}^{\infty} \left[\frac{1}{N} \sum_{n=1}^{N} R(n;\ell) \right] e^{-j2\pi f \ell T}} \qquad \text{(A-30)}$$

Comparing (A-30) with (A-17) we notice, not surprisingly, that the only difference between the two is that the periodicity of the correlation function caused by the cyclostationary behavior of the sequence $\{a_n\}$ must be "averaged out" before taking the discrete Fourier transform.

Power Spectral Density of a Synchronous Data Stream Generated by a Binary, Nonzero Mean, Cyclostationary Sequence

When the generating sequence $\{a_n\}$ is not zero mean, then the spectrum of the corresponding synchronous data stream will have a discrete component in addition to the customary continuous component. An example of a situation where this might occur is at the output of a convolutional encoder whose input is random but not equiprobable binary data. The procedure for handling this case is as follows:

Define the zero mean cyclostationary sequence $\{A_n\}$ by

$$A_n = a_n - \bar{a}_n \tag{A-31}$$

which has the properties

$$\overline{A_n} = 0$$

$$\overline{A_n A_m} = R_A(n\,;\, m-n) \tag{A-32}$$

Then, using the results of the previous section, the continuous component of the power spectrum $S_c(f)$ for a synchronous data stream generated by $\{a_n\}$ is given by

$$\boxed{S_c(f) = S_p(f)\, S_{\overline{A}}(f)} \tag{A-33}$$

where again $S_p(f)$ is defined in (A-16) and

$$\boxed{S_{\overline{A}}(f) = \sum_{\ell=-\infty}^{\infty} \left[\frac{1}{N} \sum_{n=1}^{N} R_A(n\,;\,\ell) \right] e^{-j2\pi f \ell T}} \tag{A-34}$$

The discrete spectral component $S_d(f)$ is found from

$$S_d(f) = \mathcal{F}\left\{ \left\langle \sum_n \sum_m \overline{a_n}\, \overline{a_m}\, p(t - nT)\, p(t + \tau - mT) \right\rangle \right\} \tag{A-35}$$

Making use of the Fourier transform relation of (A-6) gives the alternate form

$$S_d(f) = \int_y \sum_n \sum_m \overline{a_n}\, e^{-j2\pi ynT}\, \overline{a_m}\, e^{-j2\pi fmT}\; P(y)\, P^*(f) \left\langle e^{j2\pi(y+f)t} \right\rangle dy \tag{A-36}$$

Since by assumption $\overline{a_n}$ and $\overline{a_m}$ are both periodic with period N, then analogous to (A-26)

$$\sum_n \overline{a_n}\, e^{-j2\pi ynT} = \left[\sum_{n=1}^{N} \overline{a_n}\, e^{-j2\pi ynT}\right] \frac{1}{NT} \sum_k \delta\left(y - \frac{k}{NT}\right)$$

$$\sum_m \overline{a_m}\, e^{j2\pi fmT} = \left[\sum_{m=1}^{N} \overline{a_m}\, e^{-j2\pi ymT}\right] \frac{1}{NT} \sum_k \delta\left(f - \frac{k}{NT}\right)$$

(A-37)

Substituting (A-37) in (A-36) and integrating on y yields after simplification

$$S_d(f) = \frac{1}{NT} \sum_k \delta\left(f - \frac{k}{NT}\right) \sum_{m=1}^{N} \overline{a_m}\, e^{-j2\pi mk/N}$$

$$\times \frac{1}{NT} \sum_\ell P\left(\frac{\ell}{NT}\right) P^*\left(-\frac{k}{NT}\right) \sum_{n=1}^{N} a_n\, e^{-j2\pi n\ell/N} \left\langle e^{j2\pi(k+\ell)t/NT} \right\rangle$$

(A-38)

Performing the time average over the period NT gives as before

$$\left\langle e^{j2\pi(k+\ell)t/NT} \right\rangle = \frac{\sin \pi(k+\ell)}{\pi(k+\ell)} = \begin{cases} 1\,; & \ell = -k \\ 0\,; & \text{otherwise} \end{cases} \qquad \text{(A-39)}$$

Finally, substituting (A-39) into (A-38), and recalling that $|P(f)|^2$ is an even function of f, gives the desired result

$$S_d(f) = \frac{1}{(NT)^2} \sum_k \left|P\left(\frac{k}{NT}\right)\right|^2 \left(\sum_{m=1}^{N} \overline{a_m} e^{-j2\pi mk/N}\right) \times \left(\sum_{n=1}^{N} \overline{a_n} e^{j2\pi nk/N}\right) \delta\left(f - \frac{k}{NT}\right) \tag{A-40}$$

Note that when $\{a_n\}$ is a WSS sequences (i.e., N = 1), (A-40) reduces to the familiar result

$$S_d(f) = \frac{\left(\overline{a_1}\right)^2}{T^2} \sum_k \left|P\left(\frac{k}{T}\right)\right|^2 \delta\left(f - \frac{k}{T}\right) \tag{A-41}$$

Examples and Applications

As a simple example of a WSS sequence consider a binary, zero mean Markov source characterized by

$$\Pr\{a_{n+1} \neq a_n\} = p_t$$

$$\Pr\{a_{n+1} = a_n\} = 1 - p_t \tag{A-42}$$

The correlation function for such a source is easily shown to be

$$R(\ell) = (1 - 2p_t)^{|\ell|} \tag{A-43}$$

Substituting (A-43) into (A-17) gives

$$S_a(f) = 1 + 2 \sum_{\ell=1}^{\infty} (1 - 2p_t)^{\ell} \cos 2\pi f \ell T \tag{A-44}$$

From [6; p. 84, Eq. (454)], we have that

$$\sum_{k=1}^{n} a^k \cos k\theta = \frac{a \cos\theta - a^2 + a^{n+2} \cos(n\theta) - a^{n+1} \cos[(n+1)\theta]}{1 - 2a \cos(n\theta) + a^2} \tag{A-45}$$

which for $a < 1$ and $n \to \infty$ becomes

$$\sum_{k=1}^{\infty} a^k \cos k\theta = \frac{a \cos\theta - a^2}{1 - 2a \cos\theta + a^2} \tag{A-46}$$

Furthermore,

$$1 + 2 \sum_{k=1}^{\infty} a^k \cos k\theta = \frac{1 - a^2}{1 - 2a \cos\theta + a^2} \tag{A-47}$$

Applying (A-47) to (A-44) with $a = 1 - 2p_t$ and $\theta = 2\pi fT$, immediately gives the desired result

$$S_a(f) = \frac{1 - \left(1 - 2p_t\right)^2}{1 + \left(1 - 2p_t\right)^2 - 2\left(1 - 2p_t\right)\cos 2\pi fT}$$

$$= \frac{4p_t\left(1 - p_t\right)}{2\left(1 - 2p_t\right)\left(1 - \cos 2\pi fT\right) + 4p_t^2} \qquad \text{(A-48)}$$

Furthermore, if the data stream generated by this sequence uses rectangular pulses, i.e.

$$p(t) = \begin{cases} 1\ ; & 0 \le t \le T \\ 0\ ; & \text{otherwise} \end{cases} \qquad \text{(A-49)}$$

then, using (A-16) and (A-48)

$$\boxed{S(f) = T\,\frac{\sin^2 \pi fT}{(\pi fT)^2}\left[\frac{4p_t\left(1 - p_t\right)}{2\left(1 - 2p_t\right)\left(1 - \cos 2\pi fT\right) + 4p_t^2}\right]} \qquad \text{(A-50)}$$

This result has previously been obtained by the author using the more complex approach found in (Ref. 4; Chap. 1) and also by others (Ref. 7).

As a second example, consider the sequence formed by interleaving N independent first order Markov sources with respective transition probabilities p_{t_n} ; $n = 1, 2, \ldots$. Then, the resulting sequence is cyclostationary with correlation function

$$R(n ; \ell) = \begin{cases} \left(1 - 2p_{t_n}\right)^{\frac{|\ell|}{N}} ; & \ell = 0, \pm N, \pm 2N, \ldots . \\ 0 ; & \text{all other integer } \ell \end{cases} \qquad \text{(A-51)}$$

The power spectral density $S_a(f)$ of (A-30) is computed as (letting $\ell = kN$, $k = 0, \pm 1, \pm 2, \ldots .$)

$$S_a(f) = \frac{1}{N} \sum_{n=1}^{N} \sum_{k} \left(1 - 2p_{t_n}\right)^{|k|} e^{-j2\pi fkNT}$$

$$= \frac{1}{N} \sum_{n=1}^{N} \left\{ 1 + 2 \sum_{k=1}^{\infty} \left(1 - 2p_t\right)^k \cos 2\pi fkNT \right\} \qquad \text{(A-52)}$$

Noticing the similarity between (A-44) and (A-52) (for fixed n), we can immediately write down the result

$$S_a(f) = \frac{1}{N} \sum_{n=1}^{N} \left[\frac{4p_{t_n}\left(1 - p_{t_n}\right)}{2\left(1 - 2p_{t_n}\right)(1 - \cos 2\pi fNT) + 4p_{t_n}^2} \right] \qquad \text{(A-53)}$$

APPENDIX B

COSTAS LOOP TRACKING PERFORMANCE FOR A CONVOLUTIONALLY ENCODED SUPPRESSED CARRIER INPUT MODULATION

In this appendix, we derive the tracking performance of a Costas loop demodulator of a suppressed carrier input where the modulation is a random pulse stream with convolutionally encoded symbols. In particular, a closed form expression will be obtained for mean-square tracking jitter (or equivalently loop squaring loss) corresponding to the case where the loop arm filters are of the single pole RC type, and the data modulation is generated by the optimum rate 1/4, constraint length 3 correlated convolutional code [see (33)].

Without going into great detail, it is well known [8] that for a random pulse train [such as that characterized by (A-2)] plus additive white Gaussian noise input to a Costas loop, its (linear region) mean-square phase tracking jitter $\sigma_{2\phi}^2$ is characterized by the expression

$$\sigma_{2\phi}^2 = \frac{1}{\rho \mathscr{S}_L} \tag{B-1}$$

where* $\rho = S/N_0 B_L$ is the equivalent linear loop signal-to-noise ratio and $\mathscr{S}_L$ is the so-called "squaring loss" which is a degrading factor caused by the multiplication of in-phase and quadrature signal plus noise terms in the loop's third multiplier. More specifically, the squaring loss factor depends on the input modulation power spectrum $S_m(f)$ and the arm filter transfer function $G(j2\pi f)$ through the relationship

*Here, S denotes the average signal power, N_0 denotes the single-sided noise spectral density, and B_L denotes the single-sided loop bandwidth.

$$\mathscr{S}_L = \frac{D_m^{\,2}}{K_D D_m + \dfrac{K_L B_i T}{2R_d}} \tag{B-2}$$

where

$$D_m \triangleq \int_{-\infty}^{\infty} S_m(f) \left| G(j2\pi f) \right|^2 df \tag{B-3}$$

K_L is a constant dependent only on the filter type and is defined by

$$K_L \triangleq \frac{\displaystyle\int_{-\infty}^{\infty} \left| G(j2\pi f) \right|^4 df}{\left[\displaystyle\int_{-\infty}^{\infty} \left| G(j2\pi f) \right|^2 df\right]^2} \tag{B-4}$$

K_D is a constant dependent on both the baseband data power spectrum and the filter type, i.e.

$$K_D \triangleq \frac{\displaystyle\int_{-\infty}^{\infty} S_m(f) \left| G(j2\pi f) \right|^4 df}{\left[\displaystyle\int_{-\infty}^{\infty} S_m(f) \left| G(j2\pi f) \right|^2 df\right]^2} \tag{B-5}$$

and B_i denotes the two-sided noise bandwidth of the arm filter $G(j2\pi f)$, i.e.,

$$B_i \triangleq \int_{-\infty}^{\infty} \left| G(j2\pi f) \right|^2 df \tag{B-6}$$

Furthermore, $R_d \triangleq ST/N_0$ denotes the data (symbol) signal-to-noise ratio.

For single pole RC arm filters characterized by

$$\left| G(i2\pi f) \right|^2 = \frac{1}{1 + \left(\frac{f}{f_c}\right)^2} , \tag{B-7}$$

$K_L = 1/2$ and the 3 dB cutoff frequency f_c is related to the two-sided noise bandwidth B_i by $B_i = \pi f_c$. Thus, (B-2) simplifies to

$$\mathscr{S}_L = \frac{D_m^2}{K_D D_m + \frac{\pi f_c T}{4R_d}} \tag{B-8}$$

In order to simplify (B-8) any further, we must specify the spectrum of the data modulation or equivalently the statistics of the data symbol sequence. For the optimum rate 1/4, constraint length 3 convolutional code, we have from (22) and (34) that*

$$S_m(f) = T\left(\frac{\sin \pi fT}{\pi fT}\right)^2 \left\{1 + \frac{1}{2}\left[2 \cos 2\pi fT + \cos 4\pi fT\right]\right\} \tag{B-9}$$

Substituting (B-7) and (B-9) into (B-3) and (B-5) yields after much simplification

$$D_m = 1 - \frac{1}{2\pi f_c T}\left(1 - e^{-2\pi f_c T}\right) + \frac{\left(1 - e^{-2\pi f_c T}\right)^2}{4\pi f_c T} + \frac{\left(1 - e^{-4\pi f_c T}\right)^2}{16\pi f_c T} \tag{B-10}$$

*Note that $S_m(f)$ is used here rather than $S_c(f)$ as in (22) since the modulation power spectrum in this case contains only a continuous component.

$$K_D D_m = 1 - \frac{3 - \left(3 + 2\pi f_c T\right) e^{-2\pi f_c T}}{4\pi f_c T} \qquad \text{(B-11)}$$

$$+ \left(\frac{1 - e^{-2\pi f_c T}}{2\pi f_c T} \right) \left[\frac{3}{4} - \frac{1}{4} \left(3 + 4\pi f_c T\right) e^{-2\pi f_c T} \right]$$

$$+ \left(\frac{1 - e^{-4\pi f_c T}}{8\pi f_c T} \right) \left[\frac{3}{4} - \frac{1}{4} \left(3 + 8\pi f_c T\right) e^{-4\pi f_c T} \right]$$

For an uncorrelated rate 1/4, constraint length 3 convolutional code, the tracking performance results would be equivalent to those of an uncoded data sequence (except for a frequency scale factor). Thus, (B-1) and (B-9) still apply with, however, (B-9) through (B-11) replaced by the simpler expressions

$$S_m(f) = T \left(\frac{\sin \pi f T}{\pi f T} \right)^2 \qquad \text{(B-12)}$$

$$D_m = 1 - \frac{1}{2\pi f_c T} \left(1 - e^{-2\pi f_c T} \right) \qquad \text{(B-13)}$$

$$K_D D_m = 1 - \frac{3 - \left(3 + 2\pi f_c T\right) e^{-2\pi f_c T}}{4\pi f_c T} \qquad \text{(B-14)}$$